



Pyrrolidine in Drug Discovery: A Versatile Scaffold for Novel Biologically Active Compounds

Giovanna Li Petri¹ · Maria Valeria Raimondi¹ · Virginia Spanò¹ · Ralph Holl² · Paola Barraja¹ · Alessandra Montalbano¹

Received: 2 April 2021 / Accepted: 25 July 2021

© The Author(s) 2021

Abstract

The five-membered pyrrolidine ring is one of the nitrogen heterocycles used widely by medicinal chemists to obtain compounds for the treatment of human diseases. The great interest in this saturated scaffold is enhanced by (1) the possibility to efficiently explore the pharmacophore space due to sp^3 -hybridization, (2) the contribution to the stereochemistry of the molecule, (3) and the increased three-dimensional (3D) coverage due to the non-planarity of the ring—a phenomenon called “pseudorotation”. In this review, we report bioactive molecules with target selectivity characterized by the pyrrolidine ring and its derivatives, including pyrrolizines, pyrrolidine-2-one, pyrrolidine-2,5-diones and prolinol described in the literature from 2015 to date. After a comparison of the physicochemical parameters of pyrrolidine with the parent aromatic pyrrole and cyclopentane, we investigate the influence of steric factors on biological activity, also describing the structure–activity relationship (SAR) of the studied compounds. To aid the reader’s approach to reading the manuscript, we have planned the review on the basis of the synthetic strategies used: (1) ring construction from different cyclic or acyclic precursors, reporting the synthesis and the reaction conditions, or (2) functionalization of preformed pyrrolidine rings, e.g., proline derivatives. Since one of the most significant features of the pyrrolidine ring is the stereogenicity of carbons, we highlight how the different stereoisomers and the spatial orientation of substituents can lead to a different biological profile of drug candidates, due to the different binding mode to enantioselective proteins. We believe that this work can guide medicinal chemists to the best approach in the design of new pyrrolidine compounds with different biological profiles.

Keywords Pyrrolidine · Anticancer and antibacterial agents · Central nervous system diseases · Antidiabetics · Anti-inflammatory and analgesic agents

✉ Maria Valeria Raimondi
mariavaleria.raimondi@unipa.it

Extended author information available on the last page of the article

Abbreviations

5-LOX	5-Lipoxygenase
A549	Lung cancer cell line
AChE	Acetylcholinesterase
AD	Alzheimer's disease
AG	α -Glucosidase
ALR2	Aldose reductase
APP	Amyloid precursor protein
AR	Androgen receptor
ATX	Autotaxin
AZA	Acetazolamide
A β	Amyloid- β
BACE1	Beta-secretase 1
BBB	Blood-brain barrier
BChE	Butyrylcholinesterase
BHK	Baby hamster kidney cell line
CAPAN-1	Pancreatic cancer cell line
Cas	Carbonic anhydrases
CC ₅₀	Concentration required to inhibit cell proliferation by 50%
CCRF-CEM	Acute lymphocytic leukemia
CNS	Central nervous system
COX-1	COX-2, cyclooxygenase-1, cyclooxygenase-2
DHFR	Dihydrofolate reductase
DNJ•HCl	Deoxynojirimycin chlorohydrate
DOS	Diversity-oriented synthesis
DPP4	Dipeptidyl peptidase-4
α/γ EC ₅₀	α/γ Half maximal effective concentration values
ED ₅₀	Median effective dose
ER	Efflux ratio
ER	Estrogen receptor
ES-2	Ovarian clear carcinoma cell
FAAH	Fatty acid amide hydrolase
FDA	Food and Drug Administration
FPA	Fluorescence polarization assay
FTase	Human protein farnesyltransferase
GI ₅₀	Growth inhibitory dose 50%
Glc-N-6P	Glucosamine-6-phosphate synthase
GLP-1	Glucagon-like peptide-1
GlyT1	Glycine transporter-1
hCA I and II	Human isoenzymes I and II
HDAC2	Histone deacetylase 2
HeLa	Cervix carcinoma
hGLYT1	Human glycine transporter-1
IC ₅₀	Half maximal inhibitory concentration value
K562	Chronic myeloid leukaemia cell line
KIT	Tyrosine-protein kinase KIT

MBH	Morita–Baylis–Hillman
Mcl-1	Myeloid cell leukemia-1
MCF-7	Breast cancer cell line
MDA-MB-436	Breast carcinoma cell line
MES	Maximal electroshock
MMP-2	-9, Matrix metalloproteinases 2, -9
NAAA	<i>N</i> -Acylethanolamine acid amidase
NBS	<i>N</i> -Bromosuccinimide
NCI	National Cancer Institute
NCI-H522	Non-small cell lung cancer
NMDA	<i>N</i> -Methyl- <i>D</i> -aspartate
NP	Natural product
PARP-1-2	Poly(ADP-ribose) polymerase-1, -2
PXR	Pregnane X receptor
PC-3	Prostatic cancer cell line
PDB ID	Protein data bank identification
P-gp	P-glycoprotein
PHB2	Prohibitin 2
PK	Pharmacokinetics
PPARs	Peroxisome proliferator-activated receptors
P-tau	Tau protein
ROR γ t	Retinoic acid-related orphan receptor γ
SAR	Structure–activity relationship
SARMs	Selective androgen receptor modulators
scPTZ	Subcutaneous pentylenetetrazole
SI	Selectivity index
VDCCs	Voltage-gated calcium channels
VGSCs	Voltage-gated sodium channels
VPA	Valproic acid

1 Introduction

The development of clinically active drugs relies increasingly on the use of heterocyclic scaffolds, many of which contain nitrogen, as evidenced by the considerable number of bioactive compounds now available [1–5]. The introduction of heteroatomic fragments in these molecules is not a random choice, considering that they are useful tools for modifying physicochemical parameters and obtaining the best ADME/Tox results for drug candidates [6, 7]. Although two-dimensional (2D) flat heteroaromatic ring scaffolds are used widely by medicinal chemists, due mainly to their easy structural modification [8, 9], heteroatomic saturated ring systems allow a greater chance of generating structural diversity [10]. This molecular complexity was defined by Lovering et al. [11] through two descriptors, the sp^3 -hybridization and number of chiral centers, both of which are essential for establishing the clinical success of new bioactive molecules. Indeed, the chemical complexity and the globular three-dimensional (3D) shape offer more opportunities to improve druggability

by modifying parameters such as solubility, lipophilicity, and other ADME properties [12]. This association was also highlighted by Ritchie et al. [13] who conducted an interesting study on a set of 19,196 molecules containing three rings with different degrees of aromaticity. Molecules with growing hetero-aliphatic character showed an increase in aqueous solubility compared with those comprising three aromatic rings. Thus, each portion of the molecules can potentially influence the balance of the physicochemical parameters, which needs to be considered when designing compounds with an optimized pharmacokinetic (PK) profile. Table 1 summarizes a comparison of some of the molecular descriptors and parameters of the pyrrolidine nucleus with that of carbocyclic cyclopentane and aromatic pyrrole. As shown in Table 1, the presence of the nitrogen atom contributes to the polarity of the molecules, producing a dipole moment (D) and a marked PSA value, which cyclopentane lacks. Although both, pyrrole and pyrrolidine, show similar polar surface area (PSA) values, only the pK_{BHX} values (pyrrole = 0.15, pyrrolidine = 2.59) take into account the strength of the H-bonds. The presence of nitrogen also affects the lipophilicity of the heterocyclic rings, as evidenced by the lower LogP values of pyrrolidine and pyrrole, and the solvent accessible surface area (SASA) FISA and FOSA values. Also interesting is the CI_{logS} value of pyrrole, which is different from the LogS, highlighting how the planarity of the aromatic ring can influence aqueous solubility.

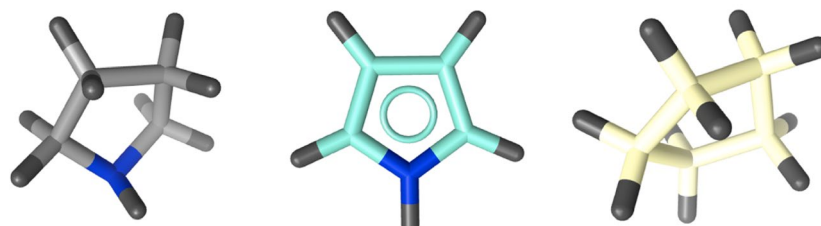
Over the past two decades, much effort have been made by industry to provide the chemistry community with new sp^3 -enriched 3D building blocks as commercial sources from which to produce molecules relevant from a medicinal chemistry point of view. In this context, Goldberg et al. [14] from AstraZeneca shed light on “design guidelines and strategic goals when designing novel reagents for drug discovery projects”, and the 3D shape appears as one of the strategic goals for the design of reagents for drug discovery programs. The 3D shapes of the non-aromatic pyrrolidine and cyclopentane rings with the aromatic pyrrole ring are compared in Fig. 1. The different bond angles and lengths clearly suggest the flatness of the 2D structure of pyrrole and the 3D coverage of pyrrolidine and cyclopentane.

A statistical analysis conducted by Tajabadi et al. [15] found that 70% of the 15,822 scaffolds belonging to natural products (NPs) are non-flat and represent an interesting resource for the design of new synthetic molecules [16]. Among such saturated ring systems, the pyrrolidine moiety is represented widely in NPs, especially in alkaloids isolated from plants or microorganisms [17–19] (Fig. 2) showing different biological activities, e.g. nicotine **1** (antioxidant, anti-inflammatory, antihyperglycemic properties), scalusamides A **2** and (*R*)-bgugaine **3** (antimicrobial, antifungal properties), 1,4-dideoxy-1,4-imino-D-ribitol **4** and aegyptolidine A **5** (anticancer properties). Therefore, it is no coincidence that the pyrrolidine nucleus is among the most preferred scaffolds in pharmaceutical science and drug design [20], as evidenced by the fact that it ranks first among the top five most common five-membered non-aromatic nitrogen heterocycles, appearing in 37 drugs approved by the United States (US) Food and Drug Administration (FDA) [21]. Moreover, pyrrolidine and its derivatives are used widely as ligands for transition metals, organocatalysts, and effective chiral controllers in asymmetric synthesis [22–24].

Table 1 Comparison of molecular descriptors and parameters of the pyrrolidine nucleus with those of carbocyclic cyclopentane and aromatic pyrrole

Molecule	D	SASA (Å ²)	FOSA	FISA	PISA	DonorHB	AcceptHB	LogPo/w	LogS	CI_LogS	pK _{BHX}	PSA
Cyclopentane	0.073	269.230	269.230	0	0	0	0	3.000	-2.642	-2.709	0	0
Pyrrolidine	1.411	258.835	225.518	33.317	0	1.000	1.500	0.459	0.854	0.809	2.59	16.464
Pyrrole	2.930	236.257	0	31.512	204.745	1.000	0.500	0.750	-0.175	-0.542	0.15	13.964

D Computed dipole moment of the molecule, SASA total solvent accessible surface area using a probe with a 1.4 Å radius, FOSA hydrophobic component of the SASA (saturated carbon and attached hydrogen); FISA, hydrophilic component of the SASA (SASA on N, O, and H on heteroatoms), PISA carbon and attached hydrogen component of the SASA, DonorHB estimated number of hydrogen bonds donated by the solute to water molecules in aqueous solution (values are averages taken over a number of configurations, so they can be non-integer), AcceptHB estimated number of hydrogen bonds accepted by the solute from water molecules in aqueous solution (values are averages taken over a number of configurations, so they can be non-integer), LogPo/w predicted octanol/water partition coefficient, LogS predicted aqueous solubility (S in mol dm⁻³ is the concentration of the solute in a saturated solution that is in equilibrium with the crystalline solid), CI_LogS conformation-independent predicted aqueous solubility, pK_{BHX} hydrogen-bond basicity scale, PSA Van der Waals surface area of polar nitrogen and oxygen atoms. Molecular descriptors and parameters were calculated using Qikprop software (version 6.2, Schrödinger, LLC, New York, NY, 2019)



MMFF94 0.647 kcal/mol MMFF94 3.287 kcal/mol MMFF94 1.549 kcal/mol

	Pyrrolidine	Pyrrole	Cyclopentane
	Bond Length (Å)		
N(1)-C(2)	1.47	1.37	-
C(1)-C(2)	-	-	1.53
C(2)-C(3)	1.51	1.38	1.52
C(3)-C(4)	1.51	1.42	1.52
C(4)-C(5)	1.52	1.38	1.52
C(5)-N(1)	1.47	1.37	-
C(5)-C(1)	-	-	1.53
	Bond Angle (Å)		
C(2)-N(1)-C(5)	107.63	109.33	-
C(2)-C(1)-C(5)	-	-	103.63
N(1)-C(2)-C(3)	105.54	108.00	-
C(1)-C(2)-C(3)	-	-	105.74
C(2)-C(3)-C(4)	102.26	107.34	106.30
C(3)-C(4)-C(5)	103.13	107.33	104.90
C(4)-C(5)-N(1)	106.83	108.00	-
C(4)-C(5)-C(1)	-	-	102.95

Fig. 1 Comparison of the three-dimensional (3D) shape of the non-aromatic pyrrolidine and cyclopentane rings with the aromatic pyrrole ring. Bond angles, bond lengths, and MMFF94 values were calculated using LigandScout software version 4.4 Expert

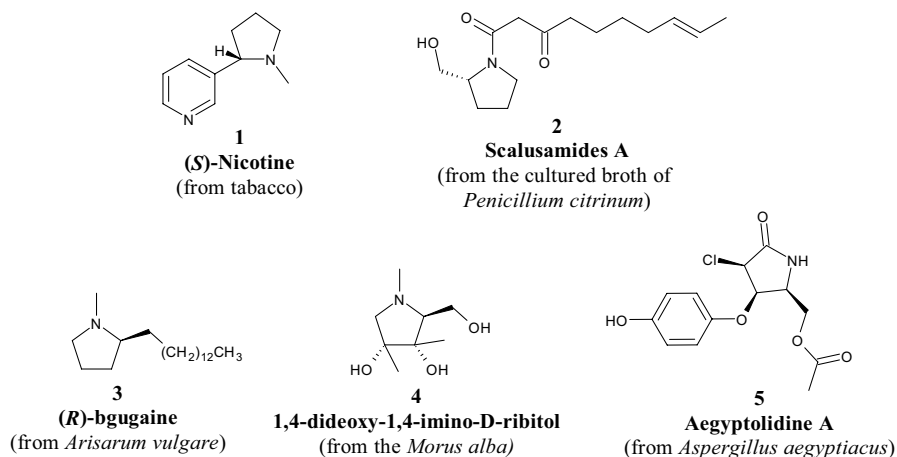


Fig. 2 Representative structures of natural alkaloids 1–5

The great interest in the pyrrolidine scaffold has allowed chemists to explore new methods for its synthesis, thus bypassing conventional approaches. The application of microwave-assisted organic synthesis (MAOS) for the synthesis of pyrrolidines has had a strong impact, allowing synthetic efficiency to be increased, and also supporting the new era of green chemistry [25].

In this review, we highlight the interest of the chemistry community in pyrrolidine and its derivatives, including pyrrolizines, pyrrolidine-2-one, pyrrolidine-2,5-diones, and prolinol, incorporated in bioactive molecules with target selectivity published from 2015 to date. We have organized the review on the basis of the synthetic approach used: (1) construction of the ring from different cyclic or acyclic precursors, and (2) functionalization of preformed pyrrolidine rings, e.g., proline derivatives.

2 Influence of Steric Factors on Biological Activity

Contrary to the parent aromatic compound pyrrole, which is a common scaffold of several bioactive compounds [26–28], the great interest in synthetic pyrrolidines is also due to the presence of up to four stereogenic carbon atoms leading to up to 16 different stereoisomers [29]. In this regard, the non-essential amino acid L-proline, with one chiral center, is frequently employed as a building block to produce chiral compounds, and as a catalyst for successful stereoselective synthesis [30, 31]. Since proteins are enantioselective, the introduction of chiral centers would represent a purposive strategy for the generation of selective ligands. Moreover, knowing the absolute and relative configuration of chiral centers can allow the toxicity or inactivity of one of the enantiomers to be avoided, a concept regulated extensively by US FDA guidelines on the “Development of new stereoisomeric drugs” [32]. In contrast to the pyrrole ring, thanks to “pseudorotation”, an intrinsic property of saturated five-membered rings, pyrrolidines gain energetically advantageous conformations offering interesting 3D coverings [33]—a useful tool for the exploration of pharmacophore space via diversity-oriented synthesis (DOS) [34, 35]. Overall, based on the electronegativity of C-4 substituents, the pyrrolidine ring of proline acquires two specific conformations called C-4 (or C γ)-exo and -endo envelope conformers. This means that puckering of the ring can be controlled easily through inductive

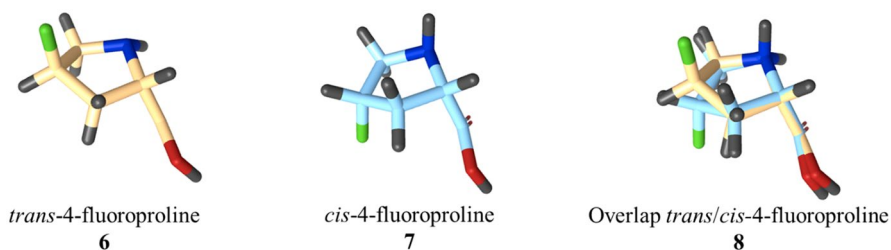


Fig. 3 Exo and endo conformers of *trans*- and *cis*-4-fluoroproline **6** and **7**, respectively; *trans/cis*-4-fluoroproline **8** resulting from the superimposition of structures **6** and **7**

and stereoelectronic factors. For instance, in the case of L-proline, the endo conformer is preferred, whereas trans-4-fluoroproline **6** and cis-4-fluoroproline **7** favor the exo and endo envelope conformation, respectively (Fig. 3). The overlap of trans/cis-4-fluoroproline **8** clearly shows the different folding of the molecules induced by the *R* or *S* configuration of the carbon bearing the fluorine atom. Conversely, C-4 alkylation of proline with a methyl or tert-butyl group is used to lock the opposite conformation [36].

2.1 The Enantiopure Compound Shows Full Agonism Towards G-Protein Coupled Receptor 40

Notably, Jurica et al. [37] synthesized a series of G-protein coupled receptor 40 (GRP40) agonists, like compounds (*R,R*)-**9** and (*S,S*)-**9**, for the treatment of type 2 diabetes (Fig. 4). They demonstrated that a cis-4-CF₃ substituent on the pyrrolidine scaffold favors the pseudo-axial conformation of the groups in the other positions, as evaluated for the acetic acid group at position 2, which is the main pharmacophore for GRP40 agonists. By lead optimization, they observed that the enantiopure (*R,R*)-**9** derivative displayed full agonism, both in human GRP40 (hGRP40, 0.11 μM) and mouse GRP40 (mGRP40, 0.054 μM) due to the different binding mode compared to its enantiomer (*S,S*)-**9** (hGRP40 0.49 μM and mGRP40 2.4 μM), in addition to a better in vivo profile in lowering glucose plasma levels in mice tested in the oral glucose tolerance test at 0.3 or 1 mg kg⁻¹ doses, and a dual mechanism of action including glucose-dependent insulin and GLP-1 secretion in vitro.

2.2 The New Spatial Arrangement in the Crystallized Ligand–Protein Complex Promotes Selectivity for CK1γ

The role of steric factors was also investigated by Luxenburger et al. [38], who synthesized potent and selective CK1 kinase inhibitors exhibiting a chiral pyrrolidine scaffold, functionalizing the CK1γ inhibitor derivative **10** (Fig. 4). Interestingly, the new enantiopure hydroxyl-functionalized pyrrolidine derivatives **11a–b** (Fig. 4) showed selectivity for CK1 in the enzyme assay against a panel of 320 different kinases. To investigate the binding mode of the chiral moiety, X-ray crystallography was conducted. The crystal structure showed that, due to the incorporation of a methylene group through a spontaneously Pictet–Spengler cyclization, two new ligands (compounds **12a,b**) (Fig. 4) were formed. These compounds showed nanomolar activity against CK1γ and CK1ε (0.011 and 0.056 μM, and 0.024 and 0.196 μM, respectively), thus suggesting that further modifications should be made to investigate how the chiral moiety influences kinase inhibition.

2.3 The Orientation of 3-*R*-Methylpyrrolidine is Responsible for a Pure Estrogen Receptor α Antagonist and Selective ER Degradator

In 2018, through biochemical and biophysical assays, coupled with high-resolution X-ray crystal structures, Fanning et al. [39] provided a molecular explanation of how

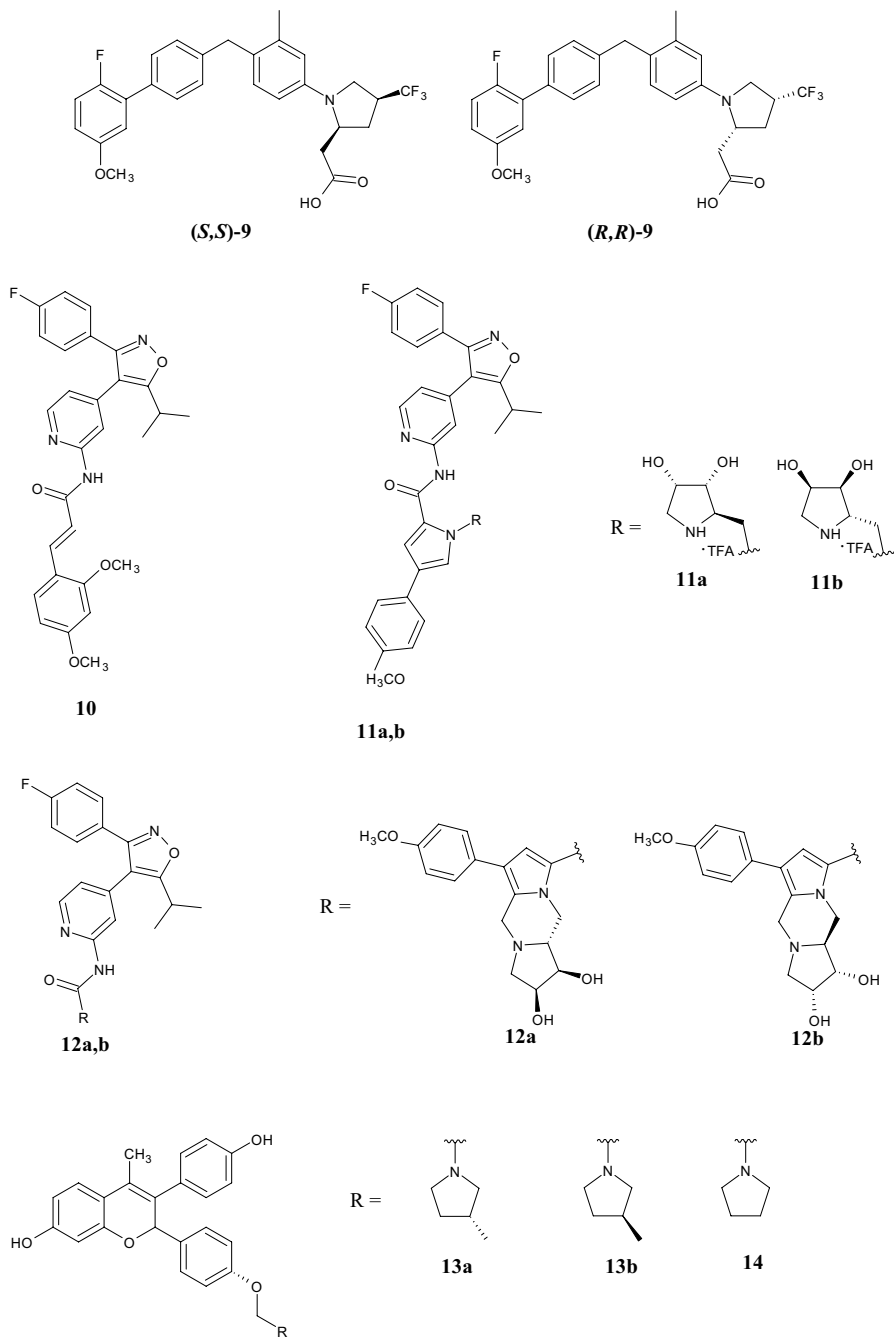


Fig. 4 Stereospecific pyrrolidine derivatives (*R,R*)-9, (*S,S*)-9, 11a,b, 12a,b, 13a,b, and 14

the stereospecific orientation can change the binding mode of antiestrogen benzo-pyran derivatives **13a,b** and **14** (Fig. 4) within the hormone-binding pocket. Specifically, they showed that the orientation of 3-*R*-methylpyrrolidine **13a** was responsible for the compound being a pure ER α (estrogen receptor α) antagonist and a selective ER degrader (PA-SERD) for the treatment of breast cancer, opposite to the 3-*S*-methylpyrrolidine **13b** and the unsubstituted derivative **14**. This is due to the capability of the *R*-methyl group of compound **13a** to increase the mobility in the loop connecting helices 11 and 12 (H11–12 loop) of the ER α protein.

2.4 Introduction of a *Cis*-3,4-Diphenylpyrrolidine Moiety Provides a Potent Inverse Agonist of ROR γ t

Recently, Jiang et al. [40] demonstrated that replacing a non-stereochemical with a stereochemical group was beneficial for the activity of a new series of *cis*-3,4-diphenylpyrrolidine derivatives as inverse agonists of the retinoic acid-related orphan receptor γ (ROR γ t)—a splice variant of the nuclear hormone receptor subfamily ROR γ involved in autoimmune diseases. The design of the new molecules started by studying the binding conformation of bicyclic sulfonamide **15** (Fig. 5), which showed excellent potency towards ROR γ t (12 nM) but suffered from undesirable activity against pregnane X receptor (PXR, EC_{50} = 144 nM, Y_{max} = 100%), which upregulates proteins involved in the detoxification and clearance of foreign toxic substances from the body. In the X-ray co-crystal structure of compound **15** in ROR γ t, the sulfonyl group assumes a pseudo-axial orientation with respect to the

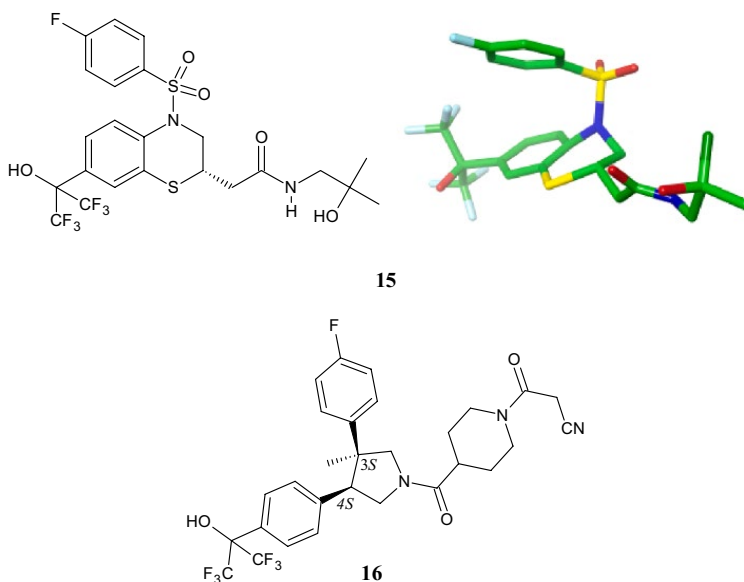


Fig. 5 Structures of retinoic acid-related orphan receptor γ (ROR γ t) ligands **15** and its ROR γ t binding conformation (top right) [40] as well as **16**

benzothiazine moiety, while the folding of the *para*-F-phenyl ring creates face-to-face *pi* stacking interactions with the benzene ring of the benzothiazine moiety, as shown in the upper panel of Fig. 5. This “U-shaped” conformation was maintained by replacing the sulphonyl group with the *cis*-3,4-diphenylpyrrolidine scaffold. Lead optimization led to piperidinyl carboxamide **16** (Fig. 5), which proved a balance between potency against ROR γ t with an EC₅₀ of 61 nM and a considerably lower PXR activity (EC₅₀=495, Y_{max}=46%). Remarkably, (1) the *cis*-configuration accommodates the two phenyl rings close to the face-to-face stacked arrangement, (2) the hexafluoroisopropyl alcohol moiety establishes a hydrogen bonding interaction between the hydroxy group and His479 of ROR γ t, (3) transposition of the C3 methyl group in C4 position leads to the loss of ROR γ t potency. In addition, (4) pyrrolidines with an unsubstituted nitrogen were weak agonists compared with tertiary amines, and (5) a *para*-F substituent in the 3-phenyl ring improved EC₅₀ values.

2.5 Basicity and Nucleophilicity of the Pyrrolidine Nucleus

While substituents at C-4 of proline affect the puckering of the ring, substituents at C-2 of pyrrolidine shift its basicity. In fact, the nitrogen atom of pyrrolidine, as a secondary amine, confers basicity to the scaffold. In this context, An et al. [41] investigated the basicity of a set of 28 pyrrolidines used as organocatalysts, showing that particularly charged substituents have a strong effect on the basicity. Lastly, due to its nucleophilicity, the pyrrolidine nitrogen represents a privileged position for substitutions, with 92% of all US FDA approved pyrrolidine drugs being substituted at the *N*-1 position [21].

2.6 Spatial Characteristics Influencing the Biological Activities of Pyrrolidine Derivatives

In summary, the advantages of using the pyrrolidine scaffold in drug design are due to the unrestricted conformation of the ring, which can be controlled and locked by the appropriate choice of substituents. Indeed, inductive and stereoelectronic factors influence the puckering of the pyrrolidine ring and, consequently, its pharmacological efficacy. The following list summarizes the spatial dispositions of the pyrrolidine scaffold that affect the biological activity towards specific targets cited in this chapter:

- *cis*-4-CF₃ substituent on the pyrrolidine scaffold endorses the pseudo-axial conformation of the groups in the other positions, leading compounds able of showing full agonism in both the human and mice GRP40 receptor;
- compared with 3-*S*-methylpyrrolidine or an unsubstituted pyrrolidine, 3-*R*-methylpyrrolidine promotes a pure ER α antagonist and selective ER degrader (PASERD) for the treatment of breast cancer;
- the introduction of a chiral pyrrolidine into molecules promotes selectivity towards CK1 receptors. However, the selectivity and potency for the CK1 γ

isoform is due to the methylene group at position 2 being involved in spontaneous intramolecular Pictet–Spilenger cyclization during crystallization with the protein;

- a *cis*-3,4-diphenylpyrrolidine scaffold gives the molecule a “U-shape” conformation that is beneficial for inverse agonistic activity on the ROR γ t receptor.

3 Pyrrolidine Derivatives Obtained by Ring Synthesis

3.1 Pyrrolidines Obtained by 1,3-Dipolar Cycloadditions

A classical method for the preparation of five-membered heterocycles is the 1,3-dipolar cycloaddition [42] between a 1,3-dipole, such as a nitron, an azide or an azomethine ylide, with a dipolarophile, typically an olefin, both of which are responsible for the regio- and stereoselectivity of the reaction [29, 43]. In particular, for synthetic pyrrolidines, the 1,3-dipolar cycloaddition reaction between nitrogen-based 1,3-dipole azomethine ylides with alkenyl dipolarophiles has been studied extensively. As shown in Fig. 6, stereoselectivity at positions 2 and 5 (R^1 and R^2) depends on the shape of the ylides, whereas stereochemistry in positions 3 and 4 correlates with the relative orientation of the substituents of the dipolarophile, leading to 3,4-*cis*- or 3,4-*trans*-substituted pyrrolidines [44].

Exploiting the 1,3-dipolar cycloaddition process between *N*-(methoxymethyl)-*N*-(trimethylsilylmethyl)benzylamine **17** and methyl acrylate **18** (Fig. 7) under acid conditions in the presence of trifluoroacetic acid (TFA), Min et al. [45] synthesized a series of benzimidazole carboxamides **19a–p** bearing the pyrrolidine nucleus at position 2. In particular, they functionalized the pyrrolidine nitrogen by introducing different aromatic rings and tested the compounds as inhibitors of poly(ADP-ribose)

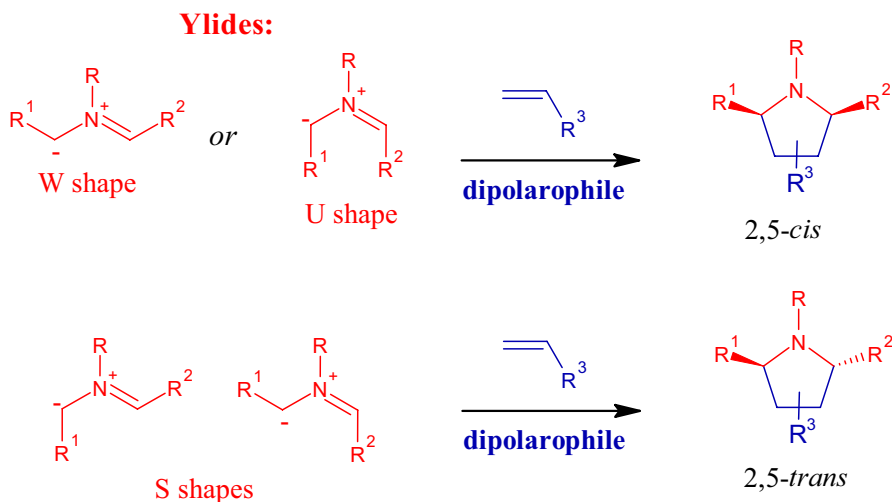
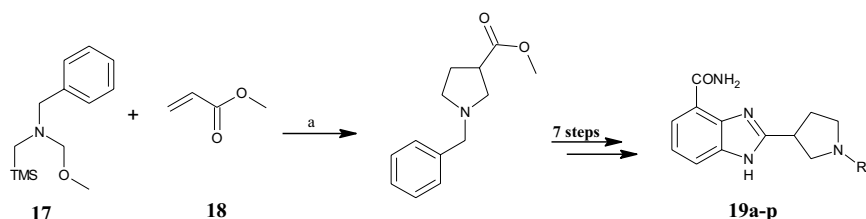


Fig. 6. 1,3-Dipolar cycloadditions to stereoselectively obtain pyrrolidine derivatives



Comp	R	PARP-1	PARP-2	PARP-1	PARP-2
		inhibition %	inhibition %	IC ₅₀ [nM]	IC ₅₀ [nM]
19a	-CH ₂ (CO)NH-phenyl	17.6	34.5	/	/
19b	-(CH ₂) ₂ (CO)NH-phenyl	19.9	41.2	/	/
19c	-(CH ₂) ₃ (CO)-phenyl	42.8	62.3	12.2	5.8
19d	-CH ₂ (CO)-phenyl	-1.1	7.2	/	/
19e	-(CH ₂) ₃ - <i>N</i> -isatin	22.0	74.5	/	/
19f	-CH ₂ CH(OH)-phenyl	5.0	9.0	/	/
19g	-(CH ₂) ₂ CH(OH)-phenyl	-2.1	6.5	/	/
19h	-(CH ₂) ₃ NH-phenyl	47.5	66.2	7.1	3.3
19i	-(CH ₂) ₂ (CO)-phenyl-4-OCH ₃	59.2	62.5	5.9	4.5
19j	-(CH ₂) ₂ (CO)-phenyl-4-Cl	65.7	65.6	3.9	4.2
19k	-(CH ₂) ₂ - <i>N</i> -isatin	6.0	37.1	/	/
19l	-(CH ₂) ₃ -NH ₂	26.8	46.4	/	/
19m	-(CH ₂) ₂ -NH ₂	24.8	32.8	/	/
19n	-(CH ₂) ₃ -NH-(CO)-phenyl	19.4	39.1	/	/
19o	-(CH ₂) ₂ -NH-(CO)-phenyl	38.4	66.2	11.1	5.7
19p	-(CH ₂) ₂ (CO)-phenyl	68.0	76.7	3.6	3.2
Veliparib	/	63.7	78.3	5.3	1.6

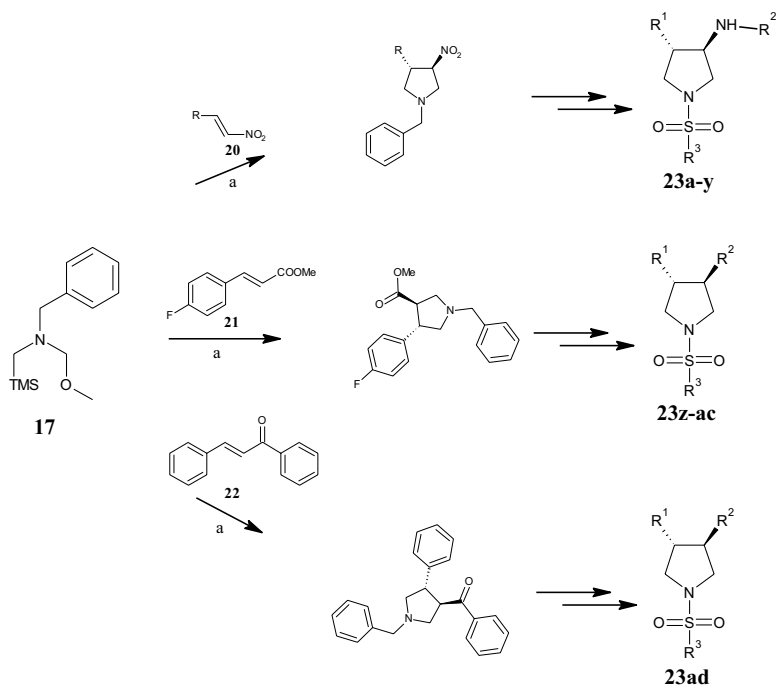
Fig. 7 General synthetic scheme to benzimidazole carboxamides **19a–p**. R substituents and poly(adenosine 5'-diphosphate (ADP)-ribose) polymerase (PARPs) inhibition assay of compounds **19a–p**. PARP-1 and -2 inhibition (%) were evaluated at 10 nM. Reagents and conditions: *a* trifluoroacetic acid (TFA), dichloromethane (DCM), 17 h, room temperature (r.t.), yield: 96%

polymerase-1 and -2 (PARP-1,-2), enzymes involved in the DNA damage repair process, as depicted in Fig. 7.

Out of 16 compounds, 6, namely **19c,h–j,o,p**, inhibited PARP-1 and -2 with IC₅₀ values ≤10 nM. Structure–activity relationship (SAR) analysis revealed that the length of the alkyl chain and the presence of the carbonyl group greatly influence biological activity. Overall, the most promising derivatives were the phenyl ketone derivatives **19c,i,j,p**, rather than the *N*-phenylamine **19h** or the *N*-benzamide **19o** derivatives. Comparing the activity within the entire class of phenyl ketone derivatives bearing 2–4 carbon atoms in the alkyl chain (**19c,d,i,j,p**), compounds **19i,j,p** with the 3-carbon atom chain were the most active. Docking studies highlighted that the phenyl ketone fragments of compounds **19j** and **19p** would bind the three important amino acid residues Gly-863, Ser-904 and Glu-988 of PARP-1, instead of only

Gly-863 and Ser-904 as in compounds **19c** and **19d**. Additionally, Van der Waals or hydrophobic interactions between the side chain of the compounds and the residues in the active site of PARP-1 were thought to facilitate the binding of these benzimidazole carboxamides. Electron donating or withdrawing groups in the para position of the benzene ring, as in compounds **19i** and **19j**, caused inhibitory activity similar to the reference compound veliparib, but with slightly higher IC_{50} values compared with the unsubstituted derivative **19p**. Reduction of the carbonyl group to a hydroxy group (**19f** and **19g**), the presence of hydrophilic amine chains (**19l** and **19m**), or the bulky phthalimide group (**19e** and **19k**), were detrimental for enzymatic inhibition. Cytotoxic assays against MDA-MB-436 (breast cancer) and CAPAN-1 (pancreatic cancer) cell lines confirmed **19j** as the most promising compound (IC_{50} 17.4 and 11.4 μ M, respectively), followed by **19p** (IC_{50} 19.8 and 15.5 μ M, respectively), which had IC_{50} values much lower than those of the reference compounds olaparib (IC_{50} 30.2 and 100 μ M, respectively, in MDA-MB-436 and CAPAN-1 cells) and veliparib (IC_{50} 100 μ M in both cell lines).

The same dipolar reagent *N*-(methoxymethyl)-*N*-(trimethylsilylmethyl)benzylamine **17** was reacted with the nitrovinyl substrate **20**, methyl trans-4-fluorocinamate **21**, and chalcone **22**, in the presence of a catalytic amount of TFA, by Wang et al. [46] to synthesize 3,4-disubstituted pyrrolidine sulfonamides **23a–y**, **23z–ac**, and **23ad**, respectively (Fig. 8). All compounds were prepared as enantiomerically pure trans isomers and tested as selective glycine transporter-1 (GlyT1) competitive inhibitors. The major role of GlyT1 is to maintain glycine concentration below saturation level at the postsynaptic ionotropic glutamatergic *N*-methyl-D-aspartate (NMDA) receptor. Since the aetiology of schizophrenia has been linked to impaired glutamatergic neurotransmission involving the NMDA receptor, the development of GlyT1 inhibitors may represent a putative treatment for it and other disorders associated with NMDA receptor hypofunction. The new pyrrolidine sulfonamides **23a–ad** were synthesized based on the SAR investigation conducted on the reference compound **23a**. The latter displayed satisfactory GlyT1 inhibitory potency in vitro, with a K_i value of 0.198 μ M, but a high efflux ratio (ER) of 8.7, indicating it as potential substrate of P-glycoprotein (P-gp)—the most relevant efflux transporter expressed in blood–brain barrier (BBB). The transformation of the sulfonamide moiety into amides, carbamides, tertiary amines, and urea groups, including the pyrrolidine nitrogen, produced inactive inhibitors of GlyT1 (structures not shown). The replacement of the benzoyl group of compound **23a** by aryl substituents (R^2) gave excellent outcomes, providing new potent analogues such as **23d,f–i,k,l,o–t,y,z** with single or double digit nanomolar activity. Among these, the anilines **23d,g–i,k,l,o,p,s,v,x** also exhibited lower ER values and consequently less susceptibility to P-gp efflux. Comparable in vitro potency and ER values were obtained when replacing the 1-methylimidazole moiety by a 1-methyl-1,2,3-triazole substituent obtaining compound **23u**, which proved metabolically unstable. As reported in Fig. 8, the fluorophenyl substituents at position 3 (R^1) of the pyrrolidine sulfonamides offered better in vitro potency and ER profile, followed by the unsubstituted phenyl ring (**23b–f**). Concerning R^2 substituents, meta-substituted derivatives showed improved biological activity. Instead, the activity of compounds with heteroaromatic substituents in position 4 (**23j,m,q,r**) was influenced by the number and position of the nitrogen atoms of the



Comp	R ¹	R ²	R ³	ER	K _i [μM]
23a	phenyl	2-Cl,3-CF ₃ -phenyl-methanone	1-CH ₃ -1 <i>H</i> -imidazol-4-yl	8.7	0.198
23b	phenyl	phenyl	1-CH ₃ -1 <i>H</i> -imidazol-4-yl	0.9	0.199
23c	phenyl	2-CH ₃ -phenyl	1-CH ₃ -1 <i>H</i> -imidazol-4-yl	1.3	1.51
23d	phenyl	3-CH ₃ -phenyl	1-CH ₃ -1 <i>H</i> -imidazol-4-yl	0.9	0.018
23e	phenyl	4-CH ₃ -phenyl	1-CH ₃ -1 <i>H</i> -imidazol-4-yl	0.6	1.25
23f	phenyl	3-CF ₃ -phenyl	1-CH ₃ -1 <i>H</i> -imidazol-4-yl	-	0.008
23g	4-F-phenyl	3-CF ₃ -phenyl	1-CH ₃ -1 <i>H</i> -imidazol-4-yl	0.9	0.003
23h	4-F-phenyl	3-Cl-phenyl	1-CH ₃ -1 <i>H</i> -imidazol-4-yl	1.1	0.003
23i	4-F-phenyl	3-CF ₃ ,4-F-phenyl	1-CH ₃ -1 <i>H</i> -imidazol-4-yl	0.8	0.005
23j	4-F-phenyl	5-CF ₃ -pyridin-3-yl	1-CH ₃ -1 <i>H</i> -imidazol-4-yl	10	1.16

Fig. 8 General synthetic scheme to pyrrolidine sulfonamides **23a–ad**. ER Efflux ratio values. K_i values towards hGLYT1 [46]. Reagents and conditions: a TFA (catalyst), DCM, r.t., overnight

heteroaromatic, as shown in Fig. 8. Finally, the analogue **23t** (R² = indanyl) showed the best balance between potency and ER value (K_i = 0.001 μM, ER = 1.5).

1,3-Dipolar cycloadditions between *N*-(methoxymethyl)-*N*-(trimethylsilylmethyl) benzylamine **17** and cis- or trans-alkenyl ester derivatives **24** (Fig. 9) in TFA, were used by Zhang et al. [47] to gain a series of 4-benzylpyrrolidine-3-carboxylic acid derivatives as potent agonists at peroxisome proliferator-activated receptors (PPARs). Among the new pyrrolidines, the cis-3*R*,4*S*-configured compounds **25** and **26** (Fig. 9) combine agonistic activity at PPARα and PPARγ, restoring glucose

23k	3-F-phenyl	3-Cl-phenyl	1-CH ₃ -1 <i>H</i> -imidazol-4-yl	1	0.042
23l	2-F-phenyl	3-Cl-phenyl	1-CH ₃ -1 <i>H</i> -imidazol-4-yl	0.9	0.021
23m	4-F-phenyl	2-CF ₃ -pyridin-4-yl	1-CH ₃ -1 <i>H</i> -imidazol-4-yl	18.5	0.118
23n	pyridin-3-yl	3-CF ₃ -phenyl	1-CH ₃ -1 <i>H</i> -imidazol-4-yl	-	0.766
23o	4-F-phenyl	3-CF ₃ -phenyl	1-CH ₃ -1 <i>H</i> -imidazol-4-yl	0.8	0.002
23p	4-F-phenyl	3-OCF ₃ -phenyl	1-CH ₃ -1 <i>H</i> -imidazol-4-yl	0.7	0.004
23q	4-F-phenyl	4-CF ₃ -pyridin-2-yl	1-CH ₃ -1 <i>H</i> -imidazol-4-yl	1.3	0.008
23r	4-F-phenyl	6-CF ₃ -pyrimidin-4-yl	1-CH ₃ -1 <i>H</i> -imidazol-4-yl	7.5	0.005
23s	4-F-phenyl	3-OCF ₃ ,4-F-phenyl	1-CH ₃ -1 <i>H</i> -imidazol-4-yl	0.7	0.002
23t	4-F-phenyl	2,3-dihydro-1 <i>H</i> -inden-1-yl	1-CH ₃ -1 <i>H</i> -imidazol-4-yl	1.5	0.001
23u	4-F-phenyl	3-CF ₃ ,4-F-phenyl	1-CH ₃ -1 <i>H</i> -1,2,3-triazole-4-yl	0.5	0.003
23v	(<i>R</i>)- esahydro-2 <i>H</i> -pyran-2-yl	3-OCF ₃ -phenyl	1-CH ₃ -1 <i>H</i> -imidazol-4-yl	0.8	0.003
23w	(<i>S</i>)-tetrahydro-2 <i>H</i> -furan-2-yl	3-OCF ₃ -phenyl	1-CH ₃ -1 <i>H</i> -imidazol-4-yl	-	0.024
23x	1,3-dioxepan-2-yl	3-OCF ₃ -phenyl	1-CH ₃ -1 <i>H</i> -imidazol-4-yl	0.9	0.002
23y	1,3-dioxan-2-y	3-OCF ₃ -phenyl	1-CH ₃ -1 <i>H</i> -imidazol-4-yl	1.1	0.002
23z	4-F-phenyl	3-OCF ₃ -phenoxyethyl	1-CH ₃ -1 <i>H</i> -imidazol-4-yl	-	0.007
23aa	4-F-phenyl	3-OCF ₃ -phenylmethanone	1-CH ₃ -1 <i>H</i> -imidazol-4-yl	1.3	0.029
23ab	4-F-phenyl	3-OCF ₃ - phenylaminomethyl	1-CH ₃ -1 <i>H</i> -imidazol-4-yl	1.2	0.060
23ac	4-F-phenyl	3-OCF ₃ -phenyl- aminomethanone	1-CH ₃ -1 <i>H</i> -imidazol-4-yl	7.2	0.36
23ad	phenyl	benzyl	1-CH ₃ -1 <i>H</i> -imidazol-4-yl	1.3	0.093

Fig. 8 (continued)

metabolism and ameliorating dyslipidaemia associated with type 2 diabetes. Compounds **25** and **26** displayed α EC₅₀ and γ EC₅₀ values in the low nanomolar range (5–90 nM). In addition, compound **26** was efficient in lowering fasting glucose and triglyceride levels in diabetic db/db mice after oral administration of a 10 mg/kg dose once daily. SAR studies revealed that (1) the oxybenzyl pyrrolidine acid series offered the best balance of PPAR α / γ functional activities, (2) the *cis*-configuration of the substituents in positions 3 and 4 of the pyrrolidine ring was preferred over the *trans* orientation, and (3) *N*-carbamoyl and *N*-aryl-substituted oxybenzyl pyrrolidine acid analogs provided potent balanced PPAR α / γ dual agonists.

Conjugated systems with biological macromolecules, including carbohydrates, lipids, proteins, and nucleic acids, require that special attention is paid to the geometry of the molecules to be combined. Unlike the pyrrolidine scaffold, spiro-pyrrolidine molecules have rigid conformations that allow for easy incorporation into biological macromolecules, including cholesterol. For this purpose, Periyasami et al. [48] synthesized a small set of novel spiro-pyrrolidine/pyrrolizines by one-pot three-component reactions. Stereo- and regioselective reactions based on 1,3-dipolar cycloaddition between the dipolarophile C3- β -cholesterolacrylate **27** (Fig. 9) under reflux in *i*PrOH for 2 h with azomethidine ylides, in turn generated in situ by reaction isatin, acenaphthoquinone, or ninhydrine with the secondary amino acids sarcosine or proline, allowed the desired compounds to be obtained as single isomers. All compounds were evaluated for their in vitro antibacterial activity

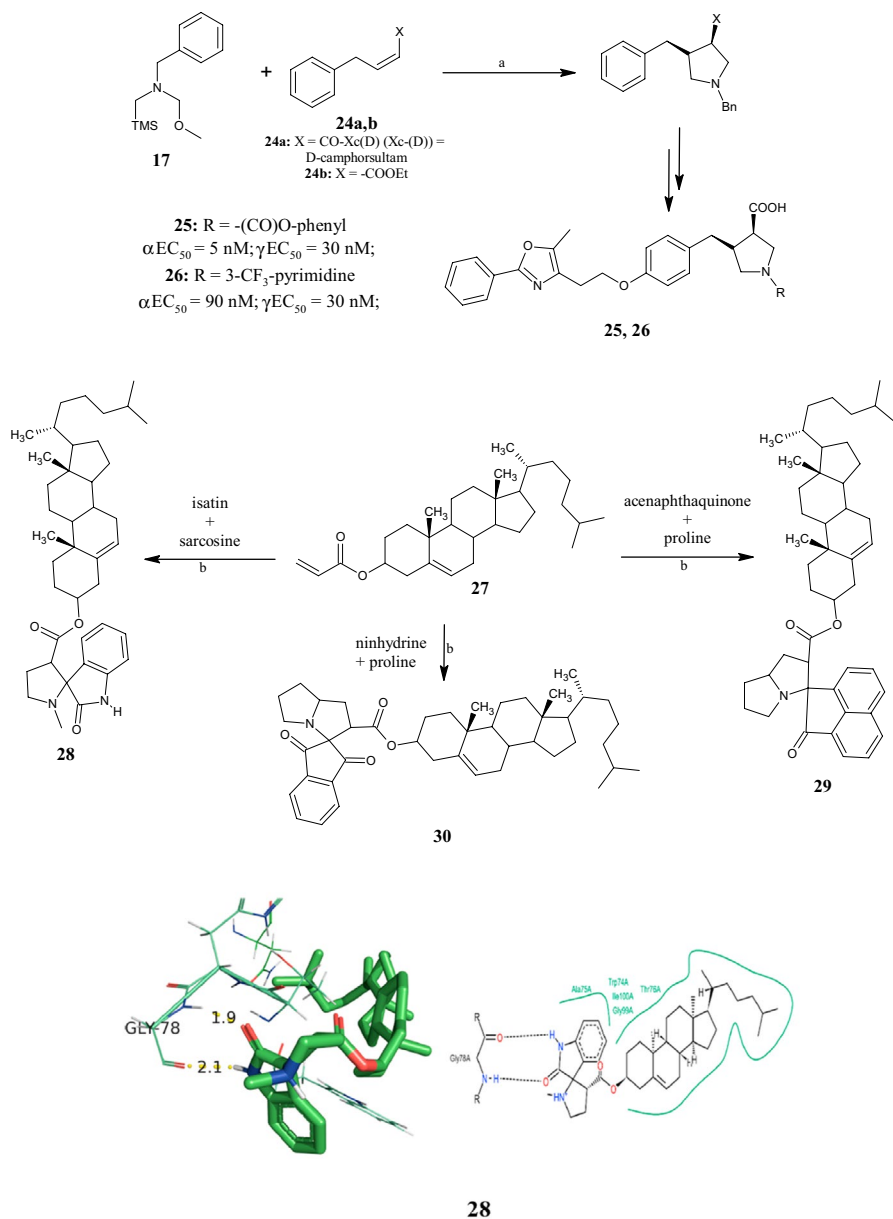


Fig. 9. 1,3-Dipolar cycloadditions to yield 4-benzylpyrrolidine-3-carboxylic acids **25** and **26**, synthesis of cholesterol-conjugated spiro-pyrrolidine/pyrrolizines **28–30**, and 3D/2D interaction diagrams of compound **28** with the active site of target receptor protein 1XFF [48]. Reagents and conditions: *a* TFA (1 M solution in DCM); *b* isopropyl alcohol (iPrOH), 2 h, under reflux, yields: 76% (**28**), 67% (**29**), 63% (**30**)

against a panel of four human pathogens, including *Vibrio cholerae*, *Proteus mirabilis*, *Micrococcus luteus*, and *Bacillus subtilis*. The most active were compounds **28**, **29**, and **30** (Fig. 9), which showed good antimicrobial activity, causing zones of growth inhibition in the performed disc diffusion assays ranging from 13.0 to 15.1 mm, at 50 µg/ml. With the aim of investigating their biological potential as glucosamine-6-phosphate synthase (Glc-N-6P) inhibitors, the authors performed *in silico* molecular docking studies with compounds **28–30** in the enzyme's active site (PDB ID: 1XFF). The results showed significant interactions with active site amino acids, revealing that the spiropyrrolidine moiety of compound **28** is engaged in two H-bond interactions involving its –NH and –CO groups with those of the aliphatic nonpolar amino acid Gly78 (Fig. 9), thus demonstrating its prominent role in the inhibition of Glc-N-6-P synthase and thus in the antibacterial activity of the compounds.

By a one-pot multicomponent approach, Shyamsivappan et al. [49] synthesized phenyl/thiophene dispiro indenoquinoxaline pyrrolidine quinolone analogues, **36a–f** and **37a–f** (Fig. 10), via 1,3-dipolar cycloaddition reaction of (*E*)-3-arylidene-8-nitro-2,3-dihydroquinolin-4(1*H*)-ones **33a–f**, ninhydrin **31**, *o*-phenylenediamine **32** and benzylamine **34**/thiophene methylamine **35** in MeOH under reflux for 2–3 h. All compounds were screened for anticancer activity against MCF-7 and HeLa cells, and only compound **37e** showed good biological activity, with IC₅₀ values of 17 and

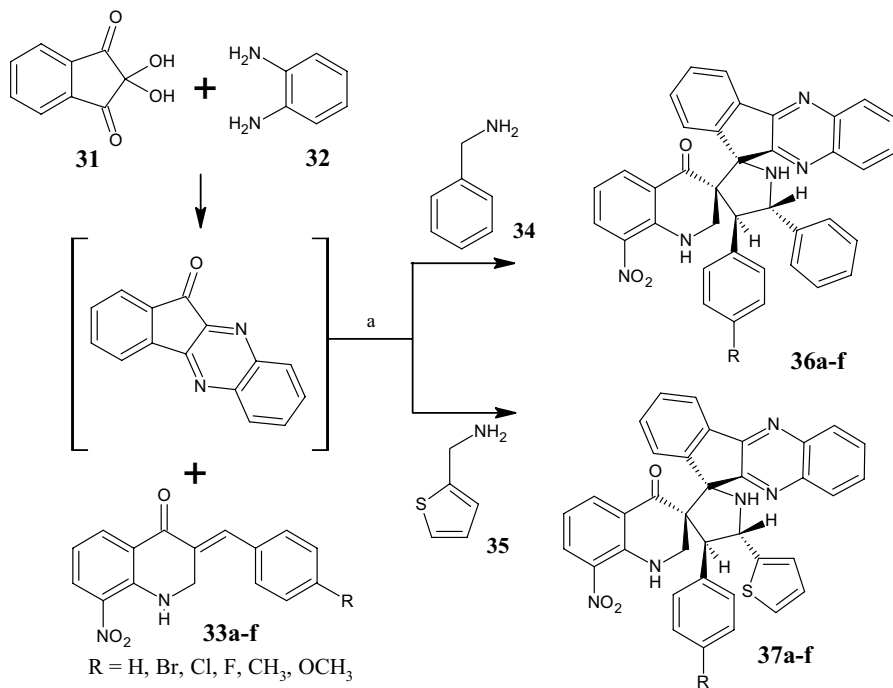


Fig. 10. 1,3-Dipolar cycloadditions to yield phenyl/thiophene dispiro indenoquinoxaline pyrrolidine quinolone derivatives **36a–f** and **37a–f**. Reagents and conditions: a MeOH, under reflux, 2–3 h, yields: 92–98% (**36a–f**) and 93–96% (**37a–f**)

19 μM , respectively, comparable to those of the reference compound doxorubicin (16 and 18 μM against MCF-7 and HeLa cells, respectively). Overall, the thiophen-containing derivatives **37a–f** showed better activity against both cell lines (IC_{50} in the range of 17 and 28 μM against MCF-7, and 19 and 30 μM against HeLa) than their respective counterparts bearing the phenyl ring **36a–f** (IC_{50} in the range of 22 and 29 μM against MCF-7; and 26 and 37 μM against HeLa). SAR analysis indicated that compounds **36e,f**, and **37e,f**, characterized by electron donating groups, such as methoxy and methyl had lower IC_{50} values than other derivatives with electron-withdrawing groups (EWGs). Further investigation into the mechanism behind the anticancer activity revealed that compound **37e** induced apoptosis through intracellular reactive oxygen species (ROS)-mediated caspase-3 activation.

3.2 Pyrrolidines Obtained by Pictet–Spengler-Oxidative Ring Contractions

Moreover, spirocyclic motifs are emerging as an interesting feature for building block with low-molecular weight in the drug discovery field [50]. In 2016, Hati et al. [51] designed and synthesized a library of spiro[pyrrolidine-3,3'-oxindoles] **38a–n** (Fig. 11) as potential anti breast cancer agents with a dual activity against histone deacetylase 2 (HDAC2) and prohibitin 2 (PHB2) enzymes. HDAC2 is responsible for the deacetylation of lysine residues on the N-terminal part of core histones (H2A, H2B, H3 and H4) and provides a tag for epigenetic repression, thus playing a significant role in transcriptional regulation, cell cycle progression, and developmental events. PHB2 acts as a mediator of transcriptional repression by nuclear hormone receptors via recruitment of histone deacetylases and works like an ER-selective co-regulator, potentiating the inhibitory activities of anti-estrogens and repressing the activity of estrogens. Based on the DOS strategy, the new compounds **38a–n** were synthesized via a one-pot Pictet Spengler-oxidative ring contraction of tryptamine, in the presence of water as reactant, mediated by stoichiometric N-bromosuccinimide (NBS) as oxidant, and a catalytic amount of TFA, varying the aromatic functionality of the pyrrole domain. Among all compounds produced, **38d,h,i** inhibited the

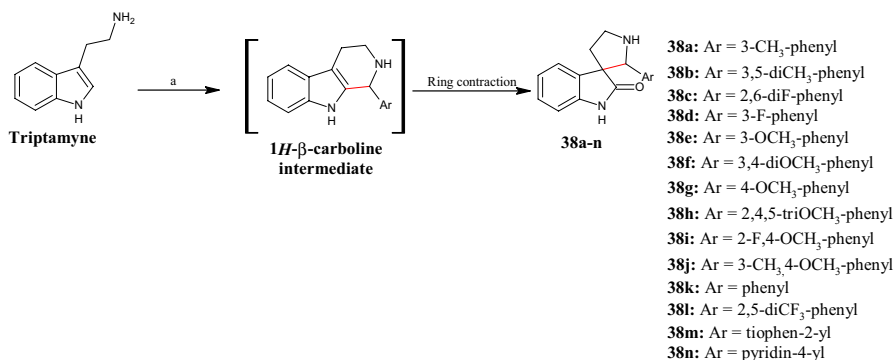


Fig. 11 General synthetic scheme to spiro[pyrrolidine-3,3'-oxindoles] **38a–n**. Reagents and conditions: *a* ArCHO, NBS, water/tetrahydrofuran (THF), TFA (cat), 0 °C to r.t., yields: 45–94%

growth of human breast cancer cell line MCF-7 by inducing apoptotic cell death at low micromolar EC_{50} values (6.00, 4.01, and 3.53 μM , respectively). Chemical proteomics indicated HDAC2 and PHB2 as potential targets of the spiro[pyrrolidine-3,3-oxindoles] and molecular docking of the most active compound **38i** with HDAC2 (PDB ID: 4LY1) confirmed probable binding interactions. Overall, based on their cytotoxic effects, compounds characterized by electron-donating or weak EWGs on the phenyl ring showed higher MCF-7 cell growth inhibition rates compared with compounds bearing one or two strong EWGs.

3.3 Pyrrolidines Obtained via Aminocyclizations

Polyhydroxylated pyrrolidines, known as aza-sugars, are considered metabolically inert carbohydrates as they mimic the oxa-carbenium transition state from carbohydrate processing enzymes. Due to their central role in different biological activities, they are emerging as attractive compounds for the treatment of cancer and metabolic diseases. In 2019, using the double reductive amination reaction, Guazzelli et al. [52] developed a series of polyhydroxylated pyrrolidines, belonging to

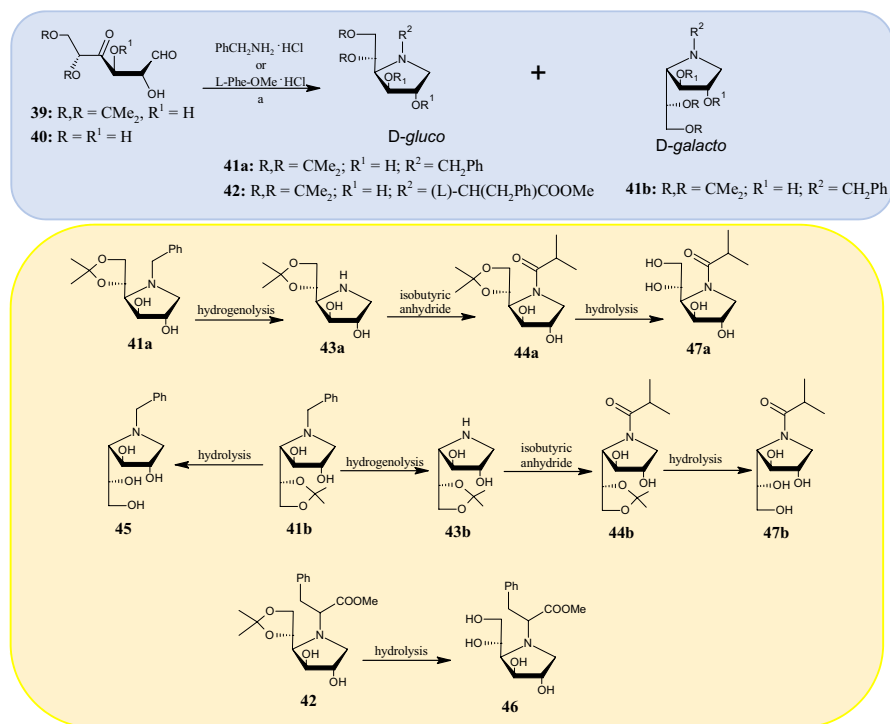


Fig. 12 *Blue panel* Synthesis of diastereoisomers **41a,b** and **42** obtained by reaction of 5,6-*O*-isopropylidene-*D*-xylo-hexos-4-ulose **39** with benzylamine hydrochloride and *L*-phenylalanine methyl ester hydrochloride, respectively. *Yellow panel* Synthesis of final compounds **43a,b**, **44a,b**, **45**, **46** and **47a,b**. Reagents and conditions: *a* sodium cyanoborohydride (NaBH₃CN), methanol (MeOH); 60 °C, 24–48 h, yields: 37% (**41a,b**), 44% (**42**)

the diastereoisomeric D-glucose and D-galactose series, as dual-target inhibitors of the enzymes α -glucosidase (AG) and aldose reductase (ALR2). Although AG represents the most important enzyme for controlling plasma sugar concentration, pathological changes in nervous, renal, vascular, and ocular systems of diabetic patients are caused by activation of ALR2. Therefore, ideal antidiabetic agents should be able to simultaneously block the catalytic activity of AG and ALR2. Aminocyclization was conducted by reacting aldohexos-4-ulose derivatives **39** and **40** (Fig. 12) with amines, including benzylamine, benzhydrylamine, ammonia, L- or D-phenylalanine methyl ester, and sodium cyanoborohydride (NaBH_3CN) as reducing agent, to obtain mixtures of D-glucose and D-galactose diastereoisomers. Among these, the authors isolated as pure compounds only diastereoisomers **41a,b** and **42** (Fig. 12) obtained by reaction of 5,6-O-isopropylidene-D-xylo-hexos-4-ulose **39** with benzylamine hydrochloride (for compounds **41a,b**) and L-phenylalanine methyl ester hydrochloride (for compound **42**). These three compounds were the starting material for the synthesis of other derivatives. Thus, through hydrogenolysis, compounds **43a,b** were obtained and were, in turn, reacted with isobutyric anhydride to give compounds **44a,b**. Finally, compounds **41b**, **42**, and **44a,b** were subjected to hydrolysis to remove the 5,6-O-isopropylidene protecting group affording compounds **45**, **46**, **47a,b**, respectively, with enhanced hydrophilic character compared with the parent compounds. Among all, the D-galacto derivative **43b** was able to reduce cell death and restore the physiological levels of oxidative stress, showing a percentage of enzyme inhibition at 100 μM of 57.1% and 30.2% against ALR2 and AG, respectively.

Recently, Li et al. [53] reported a series of (*S*)-pyrrolidines as CXCR4 chemokine receptor antagonists with antimetastatic activity. The synthesis of compounds **51a–f** (Fig. 13) was carried out in a multi-step manner in which intermediate pyrrolidine derivatives **50** were obtained by reaction of pyridin-2-yl-4-oxobutanal derivatives **48** with (*R*)-1-(4-methoxyphenyl)ethan-1-amine **49**. Among all compounds generated, **51a** with $\text{R}^1 = 3\text{-CH}_3$ showed excellent binding affinity to the CXCR4 receptor

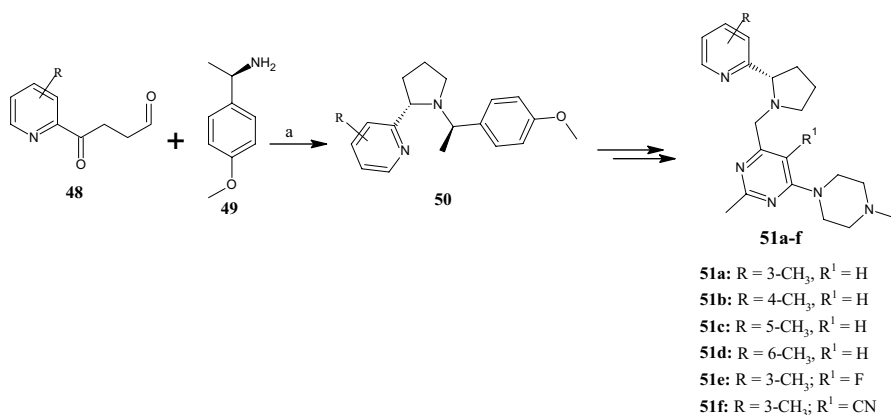


Fig. 13 General synthetic scheme to pyrrolidines **51a–f**. Reagents and conditions: *a* sodium triacetoxyborohydride [$\text{NaBH}(\text{OAc})_3$], DCM, $-70\text{ }^\circ\text{C}$ to r.t., overnight, yields: 21–45%

(IC_{50} = 79 nM competitively displacing fluorescent 12G5 antibody). Conversely, by shifting the methyl group to other positions in the pyridine ring, the IC_{50} value increased to 216, 278 and 2391 nM for compounds **51b**, **51c** and **51d**, respectively. Another feature of compound **51a** was its ability to inhibit CXCL12-induced cytosolic calcium flux (IC_{50} = 0.25 nM). In order to mitigate the overall basicity of the compounds, which can lead to issues such as hERG potassium channel inhibition, as well as CYP enzyme inhibition and phospholipidosis, the authors introduced a fluorine atom (compound **51e**) or a cyano group (compound **51f**) at the R¹ position. However, this change greatly reduced the potency of compounds **51e** and **51f**, by 4- and 7-fold, respectively. Interestingly, the antimetastatic behavior of compound **51a** was also shown in an in vivo tumor metastasis test conducted in mice, which received compound **51a** intraperitoneally at a dose of 30 mg/kg.

3.4 Pyrrolidine-2-Ones Obtained by Cyclizations

The interest in polyhydroxylated pyrrolidines led Da Silva et al. [54] to search for a short and alternative strategy to synthesize 1,4-dideoxy-1,4-imino-L-arabinitol

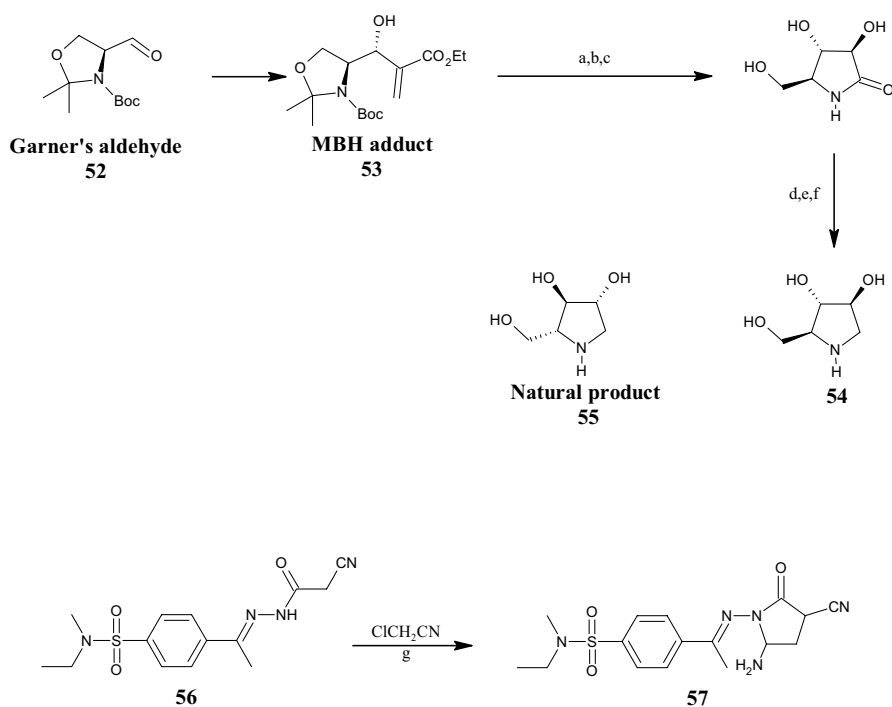


Fig. 14 General synthetic schemes to polyhydroxylated pyrrolidines **54** and pyrrolidone **57**. Reagents and conditions: *a* (1) O_3 , MeOH, $-78^\circ C$, 40 min; (2) DMS, 40 min, $-78^\circ C$ to r.t., not isolated; *b* $[Zn(BH_4)_2]$, MeOH or DCM, $-20^\circ C$, 2 h, yield: 74%; *c* TFA (2 equiv), DCM, 1 h, yield: 74%; *d* TBSCl, imidazole, DMF, 20 h, r.t., yield: 74%; *e* BH_3 , DMS, THF, 4 h, r.t., yield: 60%; *f* tetra-*n*-butylammonium fluoride (TBAF), THF, 12 h, r.t., yield: 99%. *g* triethylamine (TEA), 1,4-dioxane, 5 h, under reflux, yield: 77%

54 (Fig. 14). Compound **54** is a polyhydroxylated pyrrolidine that is a more potent α -glycosidase (AG) inhibitor than its natural enantiomer compound **55** (Fig. 14). For this reason, compound **54** is reputed to be a potential starting point for new antidiabetic and anticancer drugs. As shown in Fig. 14, the synthetic route proposed for the synthesis of **54** comprises six steps starting from a chiral Morita–Baylis–Hillman (MBH) adduct **53**, which in turn was prepared from Garner’s aldehyde **52**. Compound **54** was obtained from an intermediate pyrrolidone, which was synthesized by a linear three-step reaction sequence involving ozonolysis of the double bond of the MBH adduct **53**, followed by a stereoselective ketone reduction using zinc borohydride [$\text{Zn}(\text{BH}_4)_2$], concomitant *N*-double deprotection/*O*-deprotection with TFA, and a final amidation reaction (cyclization). Finally, the pyrrolidone intermediate was (1) silylated to decrease water solubility, (2) reduced with borane–dimethyl sulfide, and finally, (3) *O*-deprotected with tetra-*n*-butylammonium fluoride (TBAF) to afford compound **54**.

By intermolecular cyclization reactions between 2-cyanoacetamide derivative **56** and chloroacetonitrile, in the presence of triethylamine (TEA), under reflux in 1,4-dioxane for 5 h, Debbabi et al. [55] synthesized a series of *N*-ethyl-*N*-methyl benzenesulfonamides. Among these, derivative **57** (Fig. 14), characterized by a 5-amino-3-cyano-2-oxopyrrolidine core, showed antiproliferative activity against MCF-7 cells in the micromolar range ($\text{IC}_{50} = 62.53 \mu\text{M}$) and absence of cytotoxicity against normal fibroblasts of baby hamster kidney cell line (BHK). By docking studies, the activity of the compound was attributed to its binding to the dihydrofolate reductase (DHFR) (PDB ID: 4DFR).

3.5 Pyrrolidine-2,5-Diones Obtained by Cyclizations

Despite many years of research, it is still not clear how anticonvulsant drugs counteract seizures, but it is known that many of them interact with voltage-gated sodium channels (VGSCs) and voltage-gated calcium channels (VDCCs) in the central nervous system (CNS). In agreement with previous studies in which pyrrolidine-2,5-dione emerged as valuable scaffold in the treatment of epilepsy [56], in 2017, Rybka et al. [57] synthesized a library of 1,3-disubstituted pyrrolidine-2,5-diones **59a–p** (Fig. 15), obtained via cyclocondensations of dicarboxylic acids **58** with the properly substituted 1-(2-aminoethyl)- and 1-(3-aminopropyl)-4-arylpiperazines, at 180 °C for 1.5 h. Derivatives **59a–p** were administered intraperitoneally to mice and screened for their anticonvulsant activity by maximal electroshock (MES) and subcutaneous pentylenetetrazole (scPTZ) seizure tests in mice. Compounds **59j,n** showed good activity in both tests (MES ED_{50} : 88.2 mg kg^{-1} and 101.5 mg kg^{-1} , respectively; scPTZ ED_{50} : 65.7 mg kg^{-1} and 59.7 mg kg^{-1} , respectively), indicating that they are able to prevent various kinds of seizures by blocking the sodium channel with higher affinity than phenytoin. SAR analysis revealed that the anticonvulsant activity is affected strongly by substituents at position 3 of the pyrrolidine-2,5-dione scaffold. By scPTZ test, 3-benzhydryl **59a–d** and 3-isopropyl **59e–h** derivatives showed the most favorable protection in the scPTZ test, whilst 3-methyl **59i–l** and unsubstituted **59m–p** derivatives were more active in the MES test. Derivatives

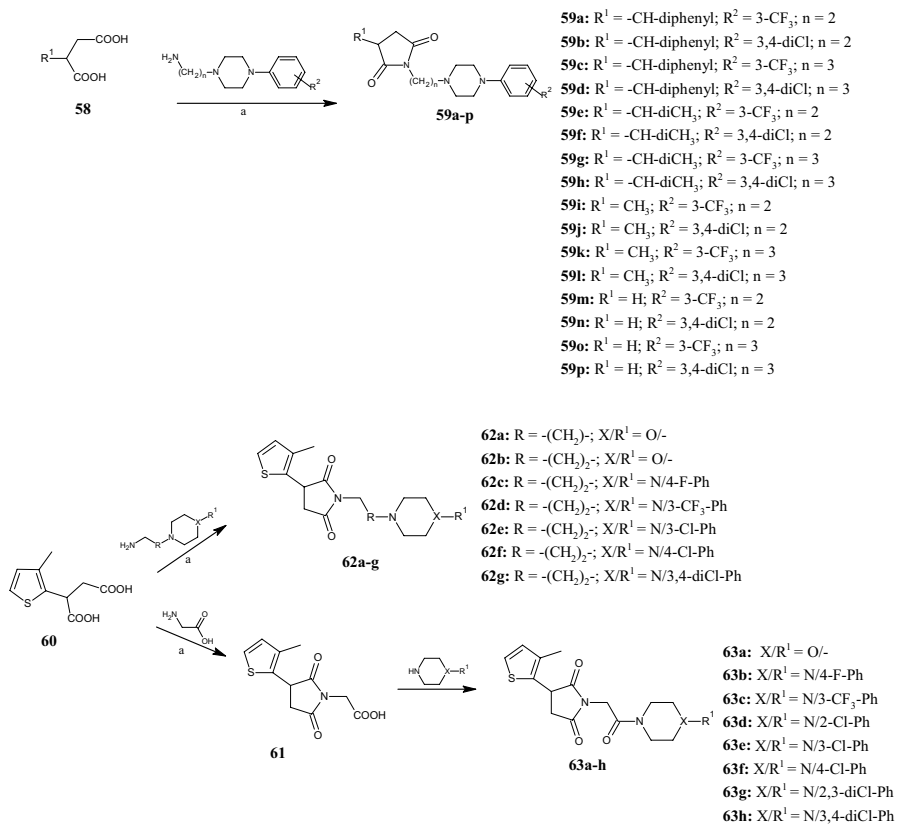


Fig. 15 General synthetic routes to pyrrolidine-2,5-diones **59a–p**, **62a–g**, and **63a–h**. Reagents and conditions: *a* 180 °C, 1.5 h., yields: 60–82% (**59a–p**), 70% (**61**), 54–86 (**62a–g**)

with a phenylpiperazine moiety bearing a 3-trifluoromethyl group were most active in the MES test, whilst 3,4-dichlorophenylpiperazines were active in both the MES and scPTZ tests. Finally, the increase in length of the alkyl chain resulted in derivatives that displayed quick onset and long-lasting anticonvulsant activity. A similar class of anticonvulsant and antinociceptive agents was also synthesized recently by Góra et al. [58], who designed hybrid derivatives of pyrrolidine-2,5-dione with the thiophene ring, compounds **62a–g** and **63a–h** (Fig. 15). While compounds **62a–g** were obtained by the reaction of 2-(3-methylthiophen-2-yl)succinic acid **60** with aminoalkylmorpholine or 1-(3-aminopropyl)-4-phenylpiperazine in one step, derivatives **63a–h** were obtained in two steps by the reaction of 2-(3-methylthiophen-2-yl)succinic acid **60** with aminoacetic acid to give intermediates **61**, which, in turn, underwent the coupling reaction. The best anticonvulsant activity was observed with compound **62b**, which displayed an ED₅₀ value of 62.14 mg kg⁻¹ in the MES test, compared with references ethosuximide (ED₅₀ > 500 mg kg⁻¹) and valproic acid (VPA) (ED₅₀ 252.7 mg kg⁻¹), and 75.59 mg kg⁻¹ in the psychomotor seizure (6 Hz) test, compared with references ethosuximide (ED₅₀ 221.7 mg kg⁻¹) and VPA (ED₅₀

130.6 mg kg⁻¹). In addition, four of the tested compounds (**62a,b,d,g**) revealed peripheral analgesic activity in the writhing test. In particular, compound **62g** was active at a dose of 30 mg/kg, similar to aspirin at the same dose. Compounds **62d** and **62g** also showed central analgesic activity in the hot-plate test at a dose of 30 mg kg⁻¹. SAR analysis revealed that the acetamide moiety can extend anticonvulsant activity in both the MES and sPTZ tests.

Later, Obniska et al. [59] expanded the same class of pyrrolidine-2,5-diones by substituting the thiophene ring with an unsubstituted phenyl moiety. The new compounds **66a–m** (Fig. 16) were obtained by the condensation of 2-methyl-2-phenyl succinic acid **64** with 3-aminopropanoic acid to give the intermediate derivatives

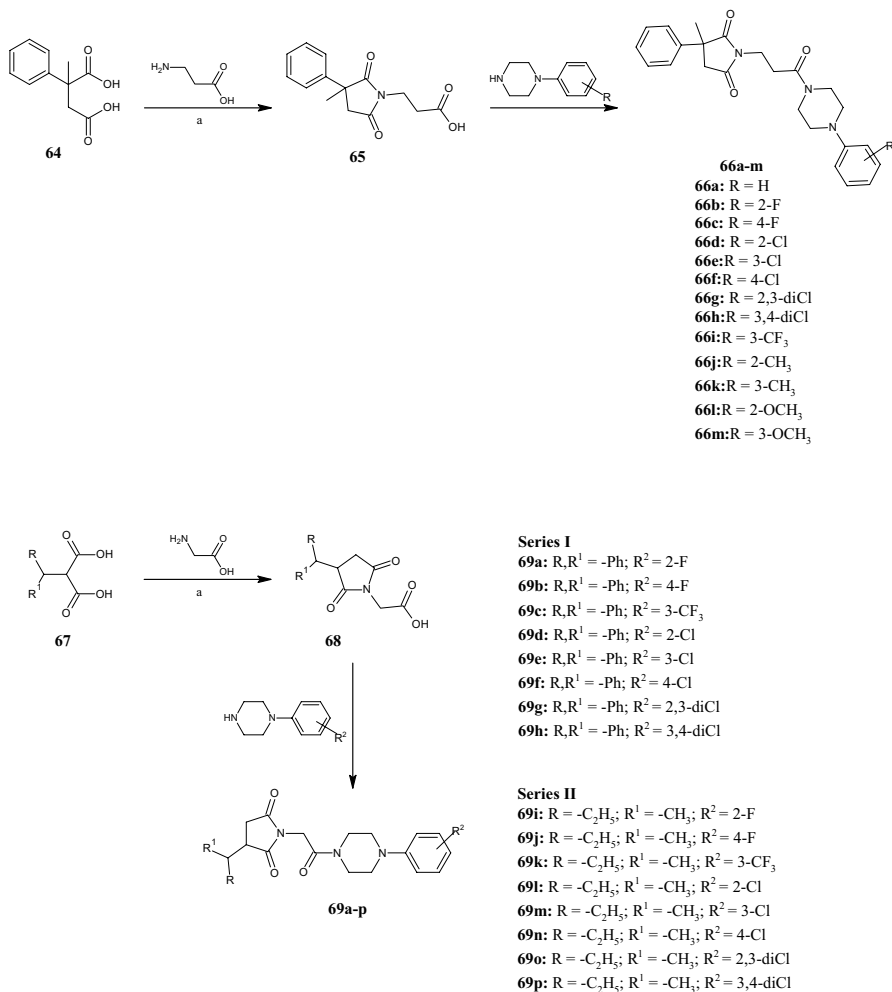


Fig. 16 General synthetic routes to pyrrolidine-2,5-diones **66a–m** and **69a–p**. Reagents and conditions: *a* 180 °C, 1 h, yields: 68% (**65**), 70% (**68**, R, R¹ = phenyl), 36% (**68**, R = methyl, R¹ = ethyl)

65, at 180 °C for 1 h. This structural change did not improve the pharmacological activity compared with the previously mentioned compound **62b**. However, the activity of the most promising derivatives **66b,c,h** was better than the reference VPA and ethosuximide, both in the MES test with ED₅₀ values of 78.3, 83.51 and 97.67 mg kg⁻¹, respectively, and in the scPTZ test, in which only compound **66b** was active (ED₅₀ 114.15 mg kg⁻¹). Finally, in 2021, Góra et al. [60] studied the anti-convulsant properties of two new series of pyrrolidine-2,5-dione-acetamides **69a-p** (Fig. 16), exhibiting a benzhydryl or *sec*-butyl group in position 3 of the pyrrolidine ring. The compounds were synthesized via intermediates **68**, which were obtained by the reaction of succinic acid derivatives **67** with aminoacetic acid at 180 °C for 1 h. Among the tested compounds, derivative **69k** showed the best ED₅₀ values of 80.38 mg kg⁻¹ in the MES and 108.80 mg kg⁻¹ in the 6 Hz tests, emerging as more effective than VPA. Summarizing the SAR analysis of this class of compounds, the activity appeared to be influenced by the substituent at position 3 of the pyrrolidine-2,5-dione ring, as well as the type of phenylpiperazine attached to the acetamide fragment. In particular, the non-aromatic substituent (*sec*-butyl) in position 3 of the pyrrolidine-2,5-dione ring and the 3-trifluoromethylphenylpiperazine fragment positively affect the anticonvulsant activity as for compound **69k**. Slightly less active than compound **69k** in the 6 Hz test was its 2-chlorophenylpiperazine analogue **69l** with a 1.2 fold higher ED₅₀ value. On the other hand, the introduction of the benzhydryl group in position 3 of the pyrrolidine-2,5-dione ring and a 4-chloro- or 2,3-dichlorophenylpiperazine fragment (compounds **69f** and **69g**) increased the activity in the scPTZ test (data not shown).

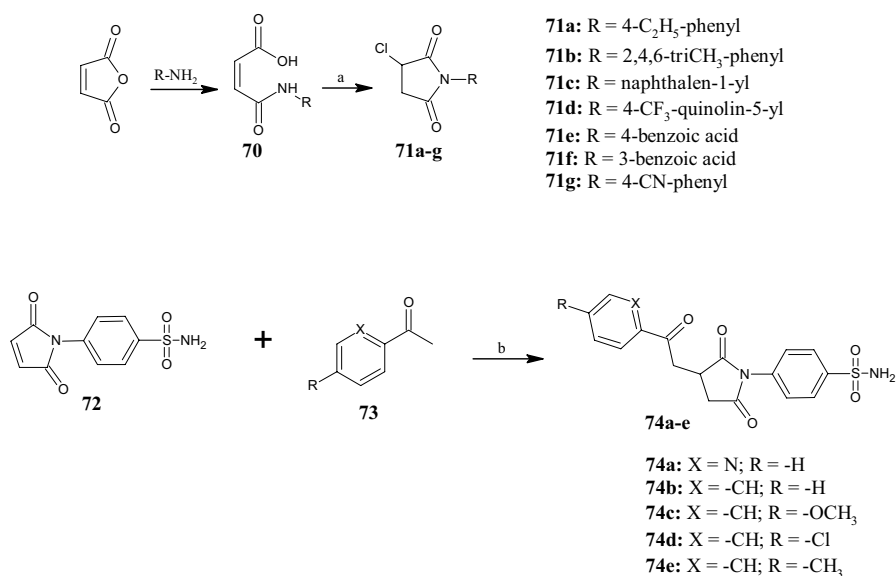


Fig. 17 General synthesis of pyrrolidine-2,5-diones **71a–g** and **74a–e**. Reagents and conditions: *a* SOCl₂, under reflux, 5–8 h, yields: 83–96%; *b* OrBU-L-threonine, 1,8-diazabicyclo[5.4.0]undec-7-ene (DBU), chloroform (CHCl₃), r.t., yields: 51.3–63.2%

Pyrrolidine-2,5-dione is a versatile scaffold, as demonstrated by Oktay et al. [61] who prepared a series of 3-chloro-1-aryl pyrrolidine-2,5-diones evaluated for their inhibitory activity on the human physiologically relevant carbonic anhydrase (CA) isoenzymes hCA I and hCA II. Both isoenzymes are involved in several diseases, such as retinal and cerebral edema, glaucoma, and epilepsy. Therefore, their inhibition could be useful to counteract these issues. The synthetic route to obtain the 3-chloro-*N*-aryl pyrrolidine-2,5-dione derivatives **71a–g** (Fig. 17) started with the reaction between maleic anhydride and aromatic amines, with consequent opening of the ring to yield (*Z*)-4-oxo-4-(arylamino)but-2-enoic acid **70**, which, in turn afforded compounds **71a–g** by reaction with thionyl chloride (SOCl₂) under reflux. All 3-chloro-1-aryl pyrrolidine-2,5-diones, except compound **71e**, were able to inhibit hCA I (K_i in the range of 23.27–36.83 nM) and hCA II (K_i in the range of 10.64 and 23.34 nM) with higher or comparable activity than the reference hCA inhibitor acetazolamide (AZA) (hCA I: K_i = 34.70 nM; hCA II: K_i = 31.93 nM). The most active compounds were derivatives **71d** (hCA I: K_i = 23.27 nM) and **71c** (hCA II: K_i = 10.64 nM), both decorated at the pyrrolidine-2,5-dione nitrogen atom with bicyclic scaffolds, such as quinoline and naphthalene.

As reported in the literature, cyclic imides, such as pyrrolidine-2,5-diones, possess interesting pharmacological properties due to the ability of the imide group to facilitate the crossing of biological membranes. Recently, Jan et al. [62] synthesized a series of pyrrolidine-2,5-dione derivatives **74a–e** (Fig. 17) as multitarget anti-inflammatory agents by applying a synthetic strategy based on Michael additions of ketones **73** to *N*-substituted maleimide **72**, at room temperature in the presence of *Ot*BU-L-threonine and 1,8-diazabicyclo[5.4.0]undec-7-ene (DBU), using a self-assembled three-component system as organocatalyst. Biological activity was determined by *in vitro* assays, such as cyclooxygenase-1 (COX-1), cyclooxygenase-2 (COX-2), and 5-lipoxygenase (5-LOX), albumin denaturation and anti-protease assays, and *in vivo* in mice. In the *in vitro* assays, all compounds showed marked COX-2 inhibition compared with the reference diclofenac (IC₅₀ = 10.05 μM) with IC₅₀ values in the range of 0.98 and 8.94 μM. The most potent compound was **74e**, which showed selectivity for COX-2 over COX-1, with a selectivity index value (SI) [SI = IC₅₀ (COX-1)/IC₅₀ (COX-2)] of 31.5. In contrast, the SI values of compounds **74a–d** were 4.88, 11.5, 18.7 and 10.9, respectively. Furthermore, aryl ketone derivatives **74a** and **74e** showed excellent inhibition of human 5-LOX with IC₅₀ values of 0.81 and 0.86 μM, respectively, which were slightly higher than the standard drug zileuton (IC₅₀ = 0.63 μM). Finally, compound **74a** also induced albumin denaturation (IC₅₀ = 5.36) and protease inhibition (IC₅₀ = 13.39 μM). The *in vivo* test with the most promising compounds **74a** and **74e** revealed anti-inflammatory activity, which was ascertained with various mediators like histamine, bradykinin, prostaglandin and leukotriene. In addition, the same compounds showed safety in an acute toxicity study, in which the lethal dose (LD₅₀) of both compounds in the experimental mice was approximately 1000 mg/kg. The SAR analysis revealed that the para-substituent on the phenyl ketone influences the biological activity. However, the replacement of the aryl ketone at position 3 of the

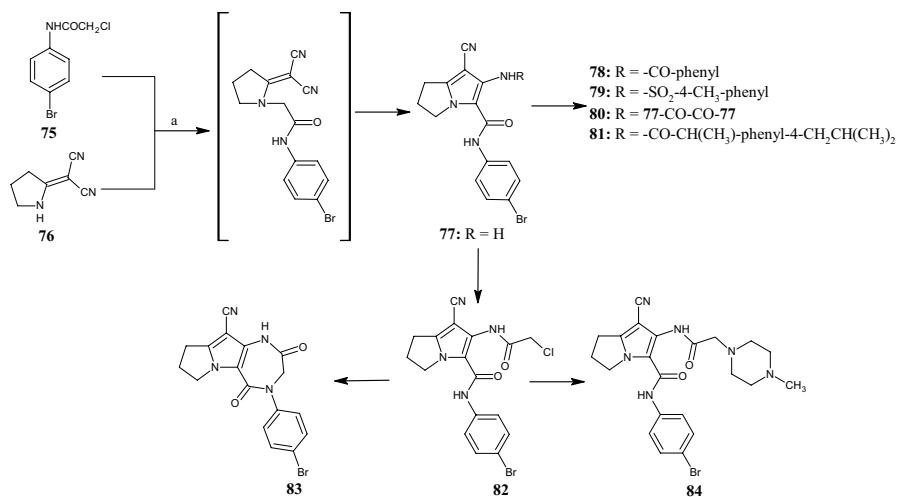


Fig. 18 General synthetic scheme to pyrrolizine carboxamide derivatives **77–84**. Reagents and conditions: a K₂CO₃, acetone, under reflux, 24 h, yields: 68% (**77**)

pyrrolidine-2,5-dione nucleus with oxocycloalkyl/oxoalkyl groups (structure not shown) was detrimental to the anti-inflammatory properties.

3.6 Pyrrolizines Obtained by Cyclizations

In 2016, Gouda et al. [63] designed and synthesized a new series of pyrrolizine carboxamides **77–84** (Fig. 18) as dual cyclooxygenase (COX) and 5-LOX inhibitors with safer gastric profile. Pyrrolizine **77** was synthesized via the intramolecular cyclization of an intermediate obtained by reacting *N*-(4-bromophenyl)-2-chloroacetamide **75** with 2-(pyrrolidin-2-ylidene)malononitrile **76** under reflux in acetone for 24 h, and was used as starting material for the synthesis of derivatives **78–84**. All pyrrolizines were assayed for anti-inflammatory activity and showed IC₅₀ values of 2.45–5.69 μM and 0.85–3.44 μM for COX-1 and COX-2, respectively. Furthermore, compound **77** exhibited higher anti-inflammatory and analgesic activities compared with ibuprofen. Upon NH₂-acylation, its analogues, such as the 2-chloroacetyl (**82**) and the benzoyl derivative (**78**) were obtained. Introduction of the 4-tolylsulfonyl moiety into compound **79** further improved both biological activities. Conversely, the hybrid compound **81**, composed of the pyrrolizine precursor **77** and ibuprofen, did not show anti-inflammatory activity and only a weak analgesic effect. 4-Methylpiperazine derivative **84**, the diazepine derivative **83**, and the dimer **80** showed lower anti-inflammatory and analgesic activities. Nevertheless, compounds **78** and **81** revealed better safety profiles than ibuprofen in acute ulcerogenicity and histopathological studies. Docking studies into COX-1 (PDB ID: 1EQG), COX-2 (PDB ID: 1CX2) and 5-LOX (PDB ID:

3O8Y, 3V99) showed that compound **79** fits well into the active sites of COX-1 and COX-2, whereas compound **79** exhibits the highest binding affinity for 5-LOX.

4 Pyrrolidine Derivatives from Commercial Building Blocks

4.1 Pyrrolidines from Proline

The interest in the pyrrolidine nucleus as skeleton of molecules with biological potential is endorsed by its similarity to the non-essential L-proline amino acid, which is used to obtain molecules with a specific stereochemistry. In 2017, Pan-nala et al. [64] developed a metal- and catalyst-free three-component decarboxylative coupling reaction of proline, aldehydes and 4-hydroxycarbazole to access pyrrolidinyl-carbazole derivatives **85a–p** (Fig. 19) with antiproliferative and antioxidant activities. The antiproliferative activity was evaluated by in vitro assays on three different cancer cell lines (MCF-7, MDA-MB-231, and lung cancer cells A549) and the results were compared with those obtained with the positive control doxorubicin. Overall, compounds **85b,c,k,p** showed the best cytotoxic activity against MCF-7 cells (IC₅₀ 8.3–16.4 μM), whereas compound **85p** was also able to reduce the growth

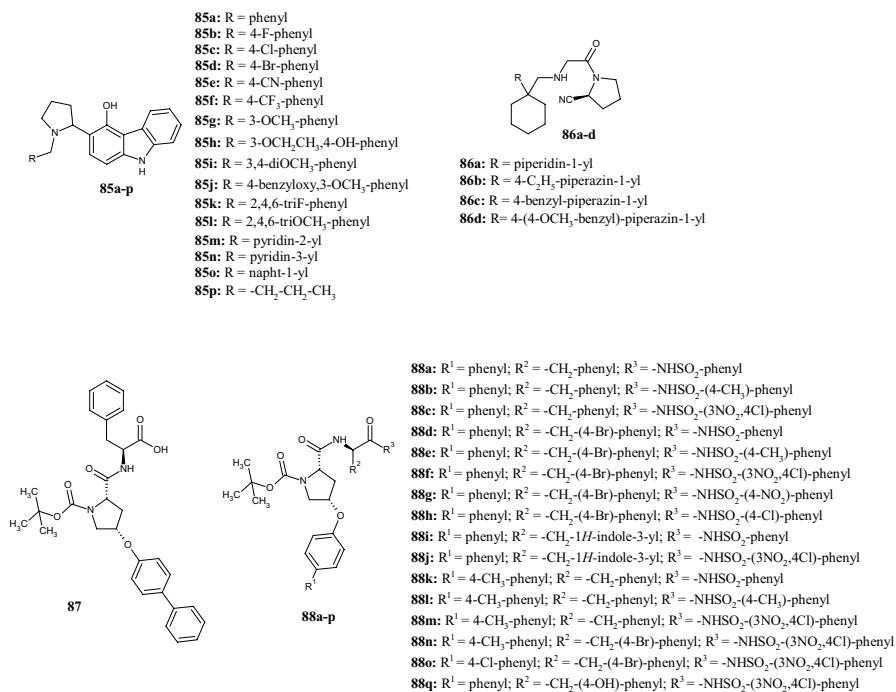


Fig. 19 Molecular structures of pyrrolidinyl-carbazole derivatives **85a–p**, pyrrolidine-2-carbonitriles **86a–d**, Mcl-1 inhibitor **87**, and pyrrolidine-1-carboxylates **88a–p**

of A549 with an IC_{50} value of 15.7 μM . Furthermore, compounds **85b,f,h,j,m** showed higher radical scavenging abilities than ascorbic acid (IC_{50} 40.9 μM), with the best results displayed by compound **85 h** (IC_{50} =27 μM) due to the presence of the hydroxy group on the phenyl ring. Docking analysis in the colchicine binding site (PDB ID: 1SA0) indicated that a methoxy-benzyloxy moiety (**85j**) and a trifluoromethyl group (**85f**) on the phenyl ring participate in hydrophobic binding interactions with several amino acid residues. Halogenated compounds **85b–d,k** displayed similar binding modes in the tubulin active site. Finally, a bulky naphthyl ring (**85o**) reduced the binding affinity.

The use of proline for the synthesis of pyrrolidine derivatives was also a strategic path for Nabil Aboul-Enein et al. [65], who synthesized a small class of antidiabetic compounds. The (*S*)-1-[(cyclohexylmethyl)glycyl]pyrrolidine-2-carbonitriles **86a–d** obtained (Fig. 19) were biologically evaluated for inhibitory activity toward dipeptidyl peptidase-4 (DPP4), a serine exopeptidase belonging to the S9B protein family, which cuts X-proline dipeptides from the N-terminus of polypeptides, such as chemokines, neuropeptides, and peptide hormones. As DPP4 is known to inactivate the incretin glucagon-like peptide-1 (GLP-1), the discovery of new DPP4 inhibitors is considered an indirect approach to increase GLP-1 levels and thus to manage diabetes mellitus type 2. The starting point for the synthesis of derivatives **86a–d** was (2*S*)-1-(chloroacetyl)pyrrolidine-2-carbonitrile, which could be obtained from *S*-proline via a chloroacetylation followed by an amidation of its carboxylate group and a final dehydration. The ability of compounds **86a–d** to inhibit the DPP4 enzyme was studied in diabetic mice that received the compounds orally at a dose of 100 mg/kg and the results were compared with those of the control group that received vildagliptin at the same dose. Serum DPP4 inhibition was evaluated 3 h after treatment. Among all, compounds **86b,c** inhibited DPP4 activity better (153% and 138%, respectively) than the control group (114%). In contrast, replacement of the piperazine ring with piperidine (**86a**) or (4-methoxybenzyl)piperazine (**86d**) reduced DPP4 inhibition to 85% and 105%, respectively. Docking studies confirmed a good binding affinity of compounds **86b,c** in the active site of DPP4 (PDB ID: 3W2T) in agreement with their anti-diabetic activity.

Starting from (2*S*,4*R*)-4-hydroxyproline, Wan et al. [66] designed and synthesized a new series of pyrrolidine derivatives based on compound **87**, which was described as potent inhibitor of myeloid cell leukemia-1 (Mcl-1) protein (K_i =8.4 μM) (Fig. 19). Using a fluorescence polarization assay (FPA), these authors observed that the most potent compounds **88a–p** were characterized by phenyl groups at R^1 , aromatic or heteroaromatic rings at R^2 , and different benzenesulfonamides at R^3 . Compounds **88c** and **88f** showed the best binding affinities towards Mcl-1, with K_i values of 0.94 and 0.53 μM , respectively, slightly higher than the positive control gossypol (K_i =0.39 μM) but very much lower than compound **87**. The replacement of phenyl or 4-bromophenyl at R^2 with 3-indolyl and *p*-hydroxyphenyl (**88i,j,p**) was unfavorable for the biological activity. Finally, the replacement of the benzenesulfonamide moiety with a hydroxy group and the introduction of linear chains or substituted phenyls instead of the 4-bromobenzyl group (structures not shown) resulted in the loss of binding affinity toward the Mcl-1 protein (K_i > 10 μM). Moreover, compound **88f** exhibited good antiproliferative activities against MDA-MB-231, PC-3 (prostate

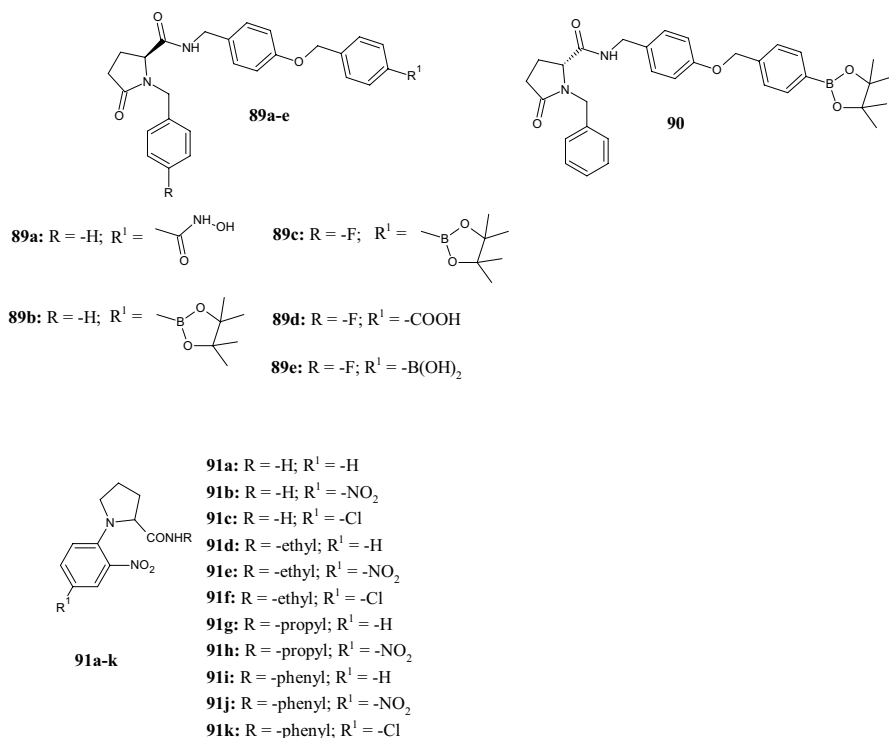


Fig. 20 Molecular structures of pyroglutamic acid derivatives **89a–e** and **90** and *N*-(2'-nitrophenyl)pyrrolidine-2-carboxamides **91a–k**

cell cancer), and K562 (chronic myeloid leukaemia) cell lines with IC₅₀ values of 13.6, 10.7, and 23.0 μM, respectively.

In 2020, Gerokonstantis et al. [67] synthesized compounds **89a–e** and **90** (Fig. 20), which are potent inhibitors of autotaxin (ATX), a glycoprotein responsible for the hydrolysis of lysophosphatidylcholine (LPC) into bioactive lipid lysophosphatidic acid (LPA), whose upregulation is involved in pathological inflammatory conditions. The main scaffolds of the new derivatives were the natural amino acid *S*-proline, the naturally derived *S*-pyroglutamic acid ((2*S*)-5-oxopyrrolidine-2-carboxylic acid), and their enantiomers. In both cases, the new derivatives possess a benzyl type substituent at the pyrrolidine nitrogen, while the carboxylic group at position 5 is coupled to side chain via an amide bond containing a benzyl-ether type substituent, which bears carboxylate, methyl ester, sulfonamide, boronic ester, imidazole, hydroxamate, tetrazole, triazol, pyridine and boronic acid moieties in para-position (structures not shown). The in vitro assay showed that the pyroglutamic acid derivatives, including hydroxamic acid **89a** (IC₅₀ 700 nM) and boronic acid derivatives **89b** (IC₅₀ 50 nM), **89c** (IC₅₀ 120 nM), **90** (IC₅₀ 180 nM), and **89e** (IC₅₀ 35 nM) were the most active compounds against

the ATX enzyme, whereas only one out of six compounds—the carboxylic acid derivative **89d**—was the least active (IC₅₀ 800 nM).

Antimicrobial peptides (AMPs) are small peptides with a wide range of inhibitory effects against bacteria and other pathogens. Pyrrocoricin, apidaecin and drosocin are some examples of proline-rich antibacterial peptide family members able to bind the bacterial DnaK protein. In 2020, Odusami et al. [68] reported the synthesis of novel *N*-(2'-nitrophenyl)pyrrolidine-2-carboxamides **91a–k** (Fig. 20) with the aim of searching for amino acid analogues with antibacterial properties capable of mimicking antimicrobial peptides. The main structural features of compounds **91a–k** were the simultaneous presence of (1) a hydrophobic group provided by the phenyl ring, and (2) a cationic charge given by the amino group after its protonation, (3) different *N'*-substituents introduced to study the effect of conformational flexibility on the antimicrobial activity. The activity was evaluated both against Gram-positive [*Bacillus subtilis* (ATCC 19659), *Enterococcus faecalis* (ATCC 14506), *Mycobacterium smegmatis* (ATCC 14468), *Staphylococcus epidermidis* (ATCC 12228) and *Staphylococcus aureus* (ATCC 25923)] and Gram-negative [*Enterobacter cloacae* (ATCC 13047), *Escherichia coli* (ATCC 25922), *Proteus vulgaris* (ATCC 33420), *Klebsiella oxytoca* (ATCC 8724) and *Proteus mirabilis* (ATCC 7002)] bacterial strains, and the results were compared with those of reference compounds streptomycin and nalidixic acid. As assessed by the minimum inhibitory concentration (MIC) values, all the carboxamides **91a–k** were more potent against *S. aureus* and *E. cloacae* than the standard streptomycin (256 µg/ml and >512 µg/ml, respectively), with compounds **91b** (15.6 µg/ml), **91c** and **91k** (62.5 µg/ml for both) being most potent against *S. aureus*, and compounds **91c** (62.5 µg/ml) and **91j** (31.3 µg/ml) being most potent against *E. cloacae*. Furthermore, the MIC values of compounds **91a–k** were lower than those found with nalidixic acid (≥500 µg/ml) against *E. faecalis*, *M. smegmatis*, *E. coli*, and *P. vulgaris* (MIC ≤250 µg/ml). Conversely, for other strains, the MICs of the carboxamides were higher than the ones of the reference compounds. SAR investigation showed that, in consideration of the *N'*-substituents, antibacterial activity increased in the order: *N'*-Et (**91d–f**) < *N'*-H (**91a–c**) < *N'*-Pr (**91g,h**) < *N'*-Ph (**91i–k**), whereas with the 4'-phenyl substituents, the activity increased in the order: 4'-PhH (**91a,d,g,i**) < 4'-PhCl (**91c** and **91f**) < 4'-PhNO₂ (**91b,e,h**) except for the *N'*-phenyl carboxamides **91i–91k**, where **91k** (4'-Cl) > **91j** (4'-NO₂) > **91i** (4'-H).

4.2 Derivatives from Other Preformed Pyrrolidine Scaffolds

Given the interest of the scientific community in the pyrrolidine nucleus, many chemical industries have synthesized variously substituted pyrrolidines as building blocks for new drugs. Among these, pyrrolidine, pyrrolidin-2-one, pyrrolidine-2,5-dione, and prolinol scaffolds are very useful preformed rings for the synthesis of new bioactive compounds.

Beta-secretase 1 (BACE1) is the enzyme responsible for the proteolytic processing of the amyloid precursor protein (APP), which leads to the generation of

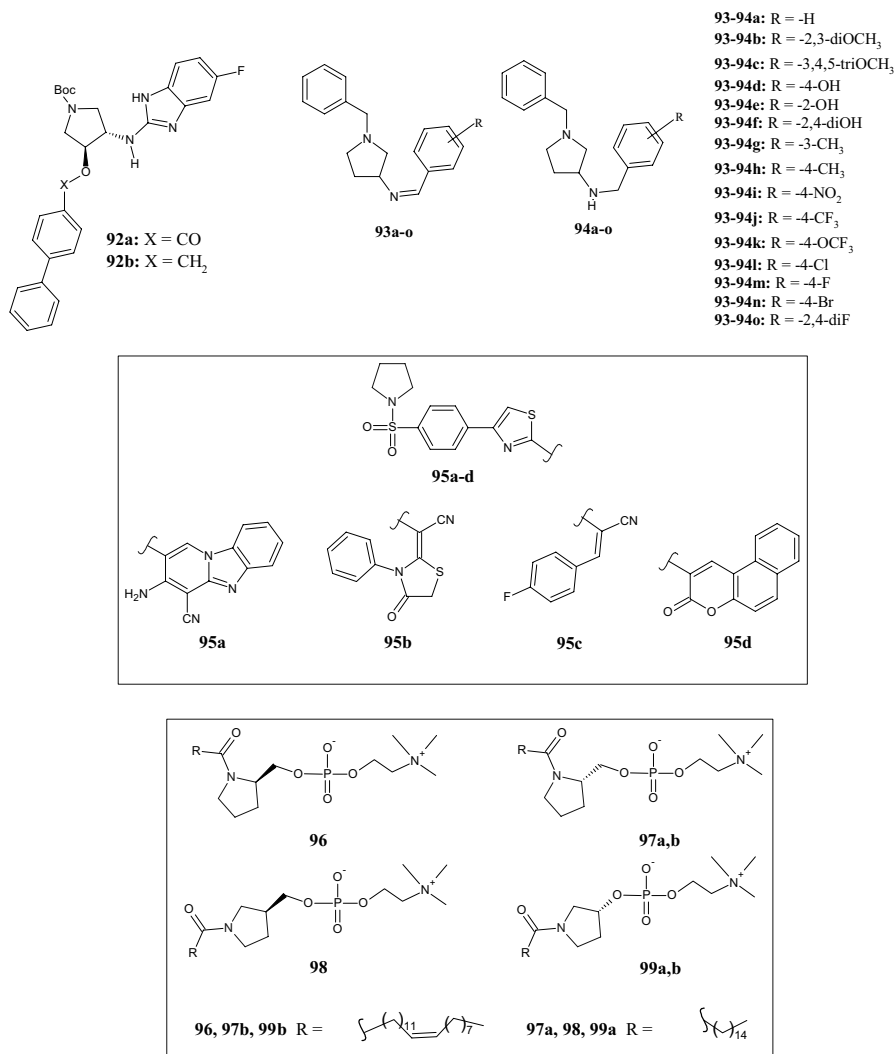


Fig. 21 Molecular structures of pyrrolidine derivatives **92a,b**, Schiff bases **93a-o** and their reduced counterparts **94a-o**, benzenesulfonylpyrrolidines **95a-d**, and pyrrolidine-based 3-deoxysphingomyelins **96, 97a,b, 98, 99a,b**

amyloid- β ($A\beta$) peptides. The aggregation of $A\beta$ in the brain of patients is responsible for the onset of Alzheimer's disease (AD). Therefore, the development of treatments towards BACE1 could be a good strategy to fight this devastating neurodegenerative disease. In 2016, De Tran et al. [69] synthesized a library of (3*S*,4*S*)-4-aminopyrrolidine-3-ol derivatives **92a,b** (Fig. 21) as potential anti-AD agents with a target selectivity toward BACE1. An in vitro inhibition assay of BACE1 showed that compound **92a** was the most active, with an IC₅₀ value of 0.05 μ M. However, when replacing the carbonyl group of **92a** with a methylene unit as in the compound

92b, the inhibition of BACE1 was approximately two times lower ($IC_{50}=0.12\ \mu\text{M}$). Unexpectedly, the opposite was observed in the cell-based assay, where compound **92b** was more effective than compound **92a**, most probably due to a difference in cell permeability (IC_{50} values 1.7 versus $40\ \mu\text{M}$, respectively). Boc-protected derivatives having the pyrrolidine nitrogen atom unsubstituted or substituted with alkyl, acyl or sulfonyl groups were less active (structures not shown). A molecular docking study confirmed interactions with the BACE1 active site.

Novel compounds for the treatment of Alzheimer's disease were also investigated by Choubey et al. [70], who synthesized multitargeted molecular hybrids of *N*-benzyl pyrrolidine derivatives, like imines **93a–o** and their reduced counterpart **94a–o** (Fig. 21). All compounds were studied for their inhibitory activity towards of cholinesterases (AChE and BChE) and BACE-1 in order to evaluate their multitarget profile. Overall, derivatives **94a–o** inhibited both cholinesterases as well as BACE-1 with greater potency than Schiff bases **93a–o**. SAR studies revealed that electron donating groups (EDGs) at the terminal phenyl ring elicit less potency with respect to acetylcholinesterase (AChE) inhibition than EWGs. Thus, derivatives bearing an EWG exhibited IC_{50} values of less than $1\ \mu\text{M}$, as observed for compounds **94k** ($0.058\ \mu\text{M}$) and **94o** ($0.069\ \mu\text{M}$), which were found to be almost as active as the reference donepezil ($0.042\ \mu\text{M}$). A similar trend was observed for butyrylcholinesterase (BChE) inhibition. All the Schiff bases, with the exception of the compound **93j** containing a 4- CF_3 group, showed a moderate inhibitory effect, whereas, among compounds **94a–o**, substitution with EWGs gave excellent BACE-1 inhibitors. Only in a few cases, such as for compounds **93j,k,o**, and **94c,d,f,i**, was the intended multitarget profile not observed.

Anticancer activity of pyrrolidine derivatives was studied by Bashandy et al. [71], who synthesized a new series of compounds characterized by the presence of a benzenesulfonylpyrrolidine moiety bearing a variously substituted 1,3-thiazole ring in position 4 of the phenyl ring. All compounds were tested for their in vitro antiproliferative activity against MCF-7 cells. Only a few compounds, namely **95a** (benzo[4,5]imidazo[1,2-*a*]pyridine), **95b** ((4-oxo-3-phenyl-1,3-thiazolidin-2-ylidene)ethanenitrile), **95c** ((4-fluorophenyl)-acrylonitrile), and **95d** (benzo[*f*]chromen-3-one) (Fig. 21), exhibited a slight improved activity compared to doxorubicin ($IC_{50}=68.6\ \mu\text{M}$), with IC_{50} values of 49.11, 48.01, 49.78 and $49.27\ \mu\text{M}$, respectively. In addition, molecular docking studies confirmed their ability to bind the DHFR active site (PDB ID: 4DFR).

In 2019, Hassan et al. [72] synthesized a series of pyrrolidine-based 3-deoxysphingomyelin analogues carrying various acyl chains (palmitoyl, palmitoleoyl, oleoyl, erucoyl, linoleoyl, and α -linolenoyl) at the pyrrolidine nitrogen atom and evaluated the compounds as antitumor agents against a panel of cancer cell lines including breast, non-small-cell lung, liver, and skin cancers. The most promising compounds were characterized by erucoyl (**96**, **97b**, **99b**) or palmitoyl (**97a**, **98**, **99a**) chains (Fig. 21). The best results were obtained for MCF-7 cells, which were more sensitive to the treatment with compounds **96**, **97b**, and **99b**, eliciting GI_{50} values at the micromolar level ($15.7\text{--}24.8\ \mu\text{M}$). This effect was also confirmed in their study on the inhibition of Akt phosphorylation. In fact, compounds **97a**, **98**, and **99a** bearing identical acyl chains but exhibiting different stereochemistry, were

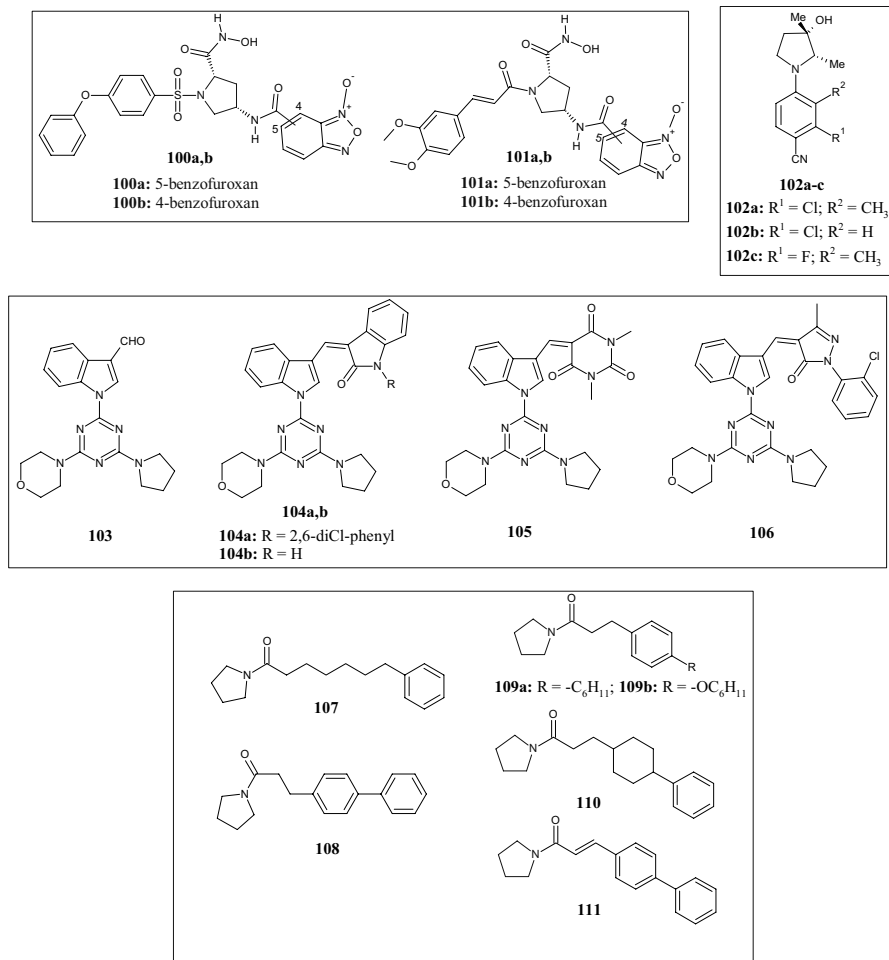


Fig. 22 Molecular structures of hybrid benzofuroxan-based pyrrolidine hydroxamates **100a,b** and **101a,b**, pyrrolidine benzonitriles **102a–c**, hybrid pyrrolidine derivatives **103**, **104a,b**, **105**, **106**, and pyrrolidine amides **107**, **108**, **109a,b**, **110**, **111**

equally active, with GI₅₀ values of 21.1, 26.4, and 32.5 μM, respectively, confirming the stereochemistry as irrelevant for activity. Molecular docking studies established that the interaction with Akt (PDB ID: 3O96) may be the predominant mechanism of action of the 3-deoxysphingomyelin analogues tested.

In 2018, Zhang et al. [73] synthesized new hybrid benzofuroxan-based pyrrolidine hydroxamates carrying on the pyrrolidine nitrogen atom two different substituents: a 3-phenoxybenzenesulfonyl (**100a,b**) or a (3,4-dimethoxyphenyl)prop-2-enyl (**101a,b**) moiety (Fig. 22). All compounds elicited antiproliferative activity against several tumor cell lines, including A549, ES-2 (ovarian clear carcinoma cell), HeLa (cervix carcinoma), K562, MCF-7, and MDA-MB-231 (IC₅₀ values of 3.56–25.64 μM), as well as NO-releasing capability (25.51–34.43 μM/l). The

anticancer activity was ascribed to the inhibition of matrix metalloproteinases 2 and 9 (MMP-2 and MMP-9), as indicated by the reduced proteolytic activity after their isolation from treated cells. Among the phenoxybenzenesulfonamides, the 5-benzofuroxan **100a** showed higher MMP-2 and -9 inhibitory activity (IC_{50} values of 102 and 162 nM, respectively) than the 4-benzofuroxan analog **100b** (IC_{50} values of 182 and 242 nM, respectively), whereas the (3,4-dimethoxyphenyl)prop-2-enamide-5-benzofuroxan (**101a**) and the 4-benzofuroxan (**101b**) were less effective (IC_{50} values of 345–524 nM). Docking studies carried out in the active site of MMP-2 (PDB ID: 1HOV) with compound **101a** highlighted the ability of the hydroxamate group to chelate the catalytic zinc ion and both arylsulfonyl and benzofuroxan groups to create hydrogen bonds with amino acid residues.

Although polyhydroxylated pyrrolidines are important scaffolds of molecules for the treatment of metabolic diseases [52, 54], hydroxy groups could be subject to oxidation and conjugation reactions that would make the molecules metabolically unstable. In this regards, with the aim of modifying the pharmacokinetic profile, Asano et al. [74] synthesized 4-(pyrrolidin-1-yl)benzotrile derivatives **102a–c** (Fig. 22) as selective androgen receptor modulators (SARMs) by optimizing the structure of previously reported 1-(4-cyano-1-naphthyl)-2,3-disubstituted pyrrolidine derivatives [75]. In particular, they introduced a methyl group at C-3 of the pyrrolidine ring that, due to its steric hindrance, should prevent metabolic instability, conferring better pharmacokinetic (PK) profiles than the parent 3-hydroxy compounds. Compounds **102b,c** had low cLogP values (<3), showed better metabolic stability, and retained potent androgen receptor (AR) agonistic activity. In addition, 2-chlorobenzotrile **102b** and 3-fluoro-2-methylbenzotrile **102c** derivatives showed good bioavailability values (53.4 and 46.3%, respectively) and strong anabolic activity in levator ani muscle (>300%), which was dose-dependent as demonstrated by in vivo studies on rats after oral administration. The X-ray co-crystal structure of **102c** bound to the AR LBD (PDB: 5T8J) highlighted a binding mode almost identical to that of the previously studied (2*S*,3*S*)-2-methyl-3-hydroxylpyrrolidine-2-chloro-3-methylbenzotrile [75].

In 2018, Kaur et al. [76] designed and synthesized a library of hybrid molecules by combining triazine-indole with morpholine/piperidine/pyrrolidine and pyrazole/pyrimidine/oxindole moieties, as novel anti-inflammatory agents. All compounds were tested for inhibition of COX-1 and COX-2 and the results were compared with that of diclofenac, a COXs non-selective inhibitor, and celecoxib, a potent and selective COX-2 inhibitor. Of all compounds tested, pyrrolidine derivatives **103,104a,b,105,106** (Fig. 22) inhibited COX-2 with IC_{50} values in the range of 1–8 μ M. The most potent was the compound **106**, characterized by a 1-(3-chlorophenyl)-3-methyl-2-pyrazolin-5-one moiety, with an IC_{50} value of 1 μ M. The SI ratio (IC_{50} COX-1/ IC_{50} COX-2) revealed compound **106** as selective for COX-2 (SI=7), compared with compounds **106,104a,b**, and **105**, which were non-selective. In addition, docking studies highlighted a well-docked pose in the COX-2 active site showing H-bond and hydrophobic interactions. Surprisingly, compound **106** also decreased formalin-induced analgesia by 69%.

N-Acylethanolamine acid amidase (NAAA) is a lysosomal hydrolase that catalyzes the degradation of *N*-acylethanolamines into fatty acids and ethanolamine in

animal tissues. Its inhibition is a therapeutic tool in several pathophysiological conditions, such as inflammation and immune disorders, as well as pain. In 2019, Zhou et al. [77] synthesized a new series of pyrrolidine amide derivatives as antiinflammatory agents and tested their selectivity towards NAAA and fatty acid amide hydrolase (FAAH), using rat NAAA (rNAAA) and rat FAAH (rFAAH) as animal model. The starting idea was to modify the linker chain and the terminal phenyl group of compounds **107** and **108** (Fig. 22), which were previously described as potent NAAA inhibitors (IC_{50} = 12.8 and 2.1 μ M, respectively). The most active compounds were **109a**, (IC_{50} = 0.5 μ M) **109b** (IC_{50} = 0.7 μ M), **110** (IC_{50} = 0.48 μ M), and **111** (IC_{50} = 1.5 μ M) (Fig. 22) showing good NAAA inhibitory effects. Conversely, no relevant activity towards FAAH was found. Studies on the chemical space on compounds **107** and **108** indicated that the activity was lost upon substitution with CH_3 , Cl, and F in position 2 of the terminal phenyl ring of parent **107**. Instead, an improvement of activity was observed upon introduction of the same substituents at positions 3 or 4 (IC_{50} 3.7–9.6 μ M), except for the 4-Cl derivative (IC_{50} 34.5 μ M) (structures not shown). The same modifications on the terminal phenyl ring of compound **108** were detrimental for activity, most probably due to the conformationally restricted chain. Isosteric replacements of the distal phenyl ring with aromatic moieties such as 2-pyridyl, 3-pyridyl, 2-thienyl, and 3-thienyl, did not improve potency. This is in contrast to the introduction of a cyclohexyl ring as in compounds **109a**

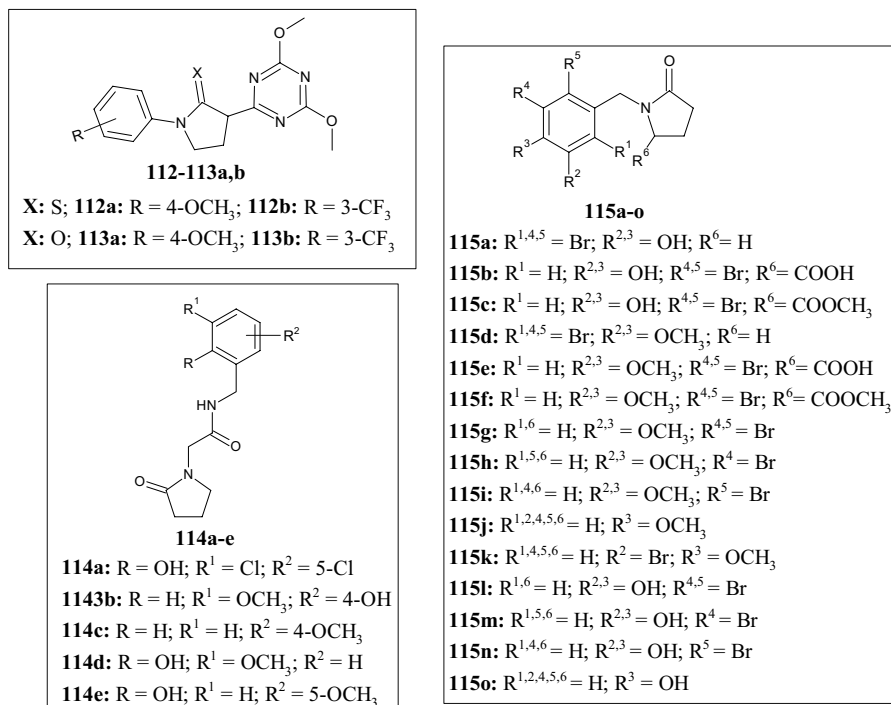


Fig. 23 Molecular structures of triazine-pyrrolidine-2-thiones **112a,b** and pyrrolidin-2-ones **113a,b**, pyrrolidin-2-ones **114a-e**, and pyrrolidin-2-ones **115a-o**

and **109b**, highlighting that (hetero)aromatic rings are less tolerated in the hydrophobic pocket of NAAA than aliphatic rings. Regarding the carbon chain between the pyrrolidine and the phenyl ring, the authors showed that flexible linkers led to a progressive increase in potency, except for compound **111**, which was well suited to the hydrophobic pocket of NAAA. Molecular docking studies (PDB ID:6DY2) suggested that **111** may inhibit NAAA via a reversible and competitive inhibition mechanism.

As analogues of isoxazole compounds, in 2019 Lucescu et al. [78] synthesized and tested triazine-pyrrolidine-2-thiones **112a,b** (Fig. 23) on the human protein farnesyltransferase (FTase). This protein catalyses the addition of a C15-farnesyl lipid group to the cysteine residue located in the carboxy-terminal tetrapeptide motif of a variety of important substrate proteins playing an important role in malignant transformations including proliferation, apoptosis, angiogenesis, and metastasis. Compound **112a** showed good inhibitory activity toward the FTase enzyme with an IC_{50} of 3.82 μM , which was approximately 11-fold lower than that of compound **112b** ($IC_{50}=41.06 \mu\text{M}$), highlighting the importance of the EWG on the phenyl ring. Interestingly, these two derivatives showed much better activity compared with the analogue in which pyrrolidine was replaced by the aromatic oxazole ring (structure not shown). In addition, the replacement of pyrrolidine-2-thione with pyrrolidin-2-one **113a,b** (Fig. 23) did not affect activity toward the FTase protein.

The pyrrolidine-2-one scaffold is a structural feature recurrent in antitumor agents, as demonstrated by Kumar et al. [79] who synthesized the novel derivatives **114a–e** (Fig. 23) by the reaction of substituted salicylaldehydes and 2-(2-oxopyrrolidin-1-yl)acetamide, leading to the respective Schiff base intermediates which were, in turn, reduced with sodium borohydride. Among all, compounds **114d** and **114e** showed the highest growth inhibition percentage against CCRF-CEM (acute lymphocytic leukemia) (**114d**=73.15%) and NCI-H522 (non-small cell lung cancer) (**114e**=41.8%) of the National Cancer Institute (NCI) panel. SAR analysis revealed that EWGs at positions 3 or 5 of the phenyl ring were unfavorable for antiproliferative activity compared with electron-donating methoxy groups. Hydroxy group introduction at position 2 (**114d** and **114e**) led to an increase in antiproliferative activity compared with compounds **114b** and **114c**. Docking analyses suggested binding to the podophyllotoxin pocket of the protein gamma tubulin (PDB ID: 1SA1) as a potential mechanism of action underlying the anticancer activity.

The versatility of the pyrrolidine-2-one scaffold was demonstrated by Rezaei et al. [80], who synthesized novel *N*-benzyl-2-pyrrolidone derivatives **115a–o** (Fig. 23) as antioxidants and inhibitors of AChE and BChE. AChE is an ubiquitous enzyme of the serine hydrolases class responsible for hydrolyzing the neurotransmitter acetylcholine, together with the homologous BChE. AD is the most common form of dementia, characterized by loss of short-term memory, spatial disorientation, progressive loss of cognitive function, decreased intellect, and some other minor expressions. A common feature of the AD is the presence of AChE, which is usually related to the A β plaques and neurofibrillary tangles in the patient's brain. Recent findings suggested that both A β and abnormally hyperphosphorylated tau protein (P-tau) may influence the AChE expression with the development of a vicious cycle of A β and P-tau dysregulation. In this context, AChE and BChE inhibitors can

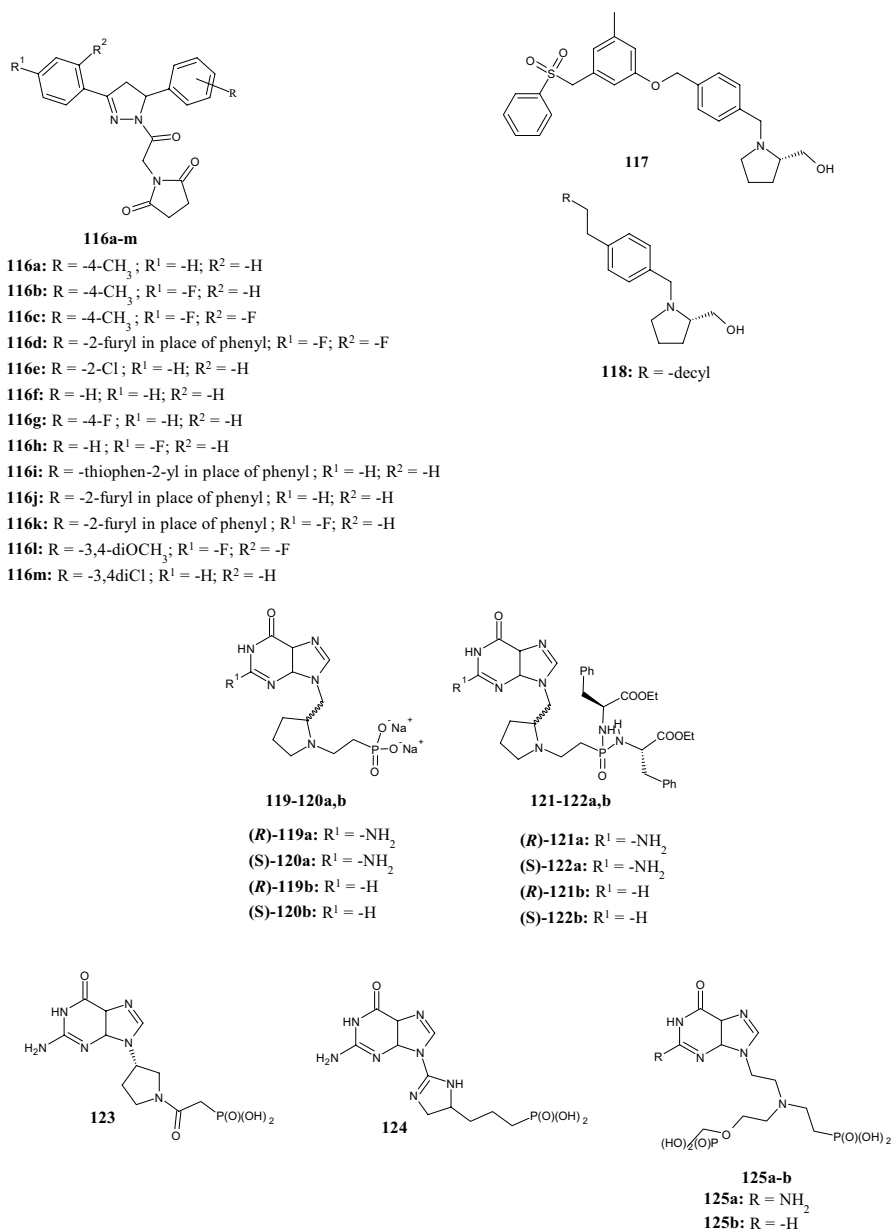


Fig. 24 Molecular structures of hybrid pyrrolidine-2,5-diones **116a-m**, 2-(hydroxymethyl)pyrrolidines **117** and **118**, pyrrolidine phosphonates **119,120a,b**, and phosphoramidate prodrugs **121,122a,b**

improve the cholinergic transmission, but with modest and temporary therapeutic effects. All compounds synthesized by the authors were able to inhibit the AChE enzyme at low nanomolar concentrations, with K_i values in the range of 2.60 and

16.36 nM. The most powerful AChE inhibitor was compound **115f** with a K_i value of 2.60 nM. Furthermore, all compounds inhibited BChE with K_i values in the range of 13.10 and 54.47 nM. Measuring the DPPH radical scavenging activity, compounds **115b,c,l-o** showed interesting antioxidant activity with half maximal radical scavenging concentrations (IC_{50} μ g/ml) in the range of 4.71 and 53.30. The radical scavenger activity is affected by the phenolic fraction and varies according to the number and position of the hydroxy groups.

To escape the problem of drug resistance, Tilekar et al. [81] recently published new pyrazoline-substituted pyrrolidine-2,5-dione hybrids **116a-m** (Fig. 24), with anticancer activity against MCF7, HT29, and K562 cancer cells. Compounds **116b,f,g**, showed nanomolar activity against MCF7 with IC_{50} values in the range of 0.42 and 0.78 μ M. Compounds **116b** and **116m** showed also activity in the sub-micromolar range against HT29 cells (IC_{50} 0.92 μ M and 0.39 μ M, respectively). The cytotoxicity assay against K562 revealed that compounds **116a** and **116g** (IC_{50} 24.74 and 31.56 μ M, respectively) were more potent than the reference compound pioglitazone (IC_{50} 40.3 μ M). Further studies with compound **116b** demonstrated its ability to reduce the cell population in the G2/M phase and increase the cell population in the G0/G1 phase, as well as inhibition of the anti-apoptotic protein Bcl-2 in a dose-dependent manner.

To obtain potent dual sphingosine kinase 1/2 (SphK1/SphK2) inhibitors, Li et al. [82] synthesized a series of 2-(hydroxymethyl)pyrrolidines, based on SAR investigation of potent and selective inhibitors previously reported in the literature (compound **117**, SphK1-selective inhibitor) (Fig. 24). These enzymes are involved in the production of sphingosine 1-phosphate (S1P) from sphingosine and ATP, in a signalling pathway that is involved in cancer progression and immune cell chemotaxis. While the 2-(hydroxymethyl)pyrrolidine scaffold is essential for hydrogen bonding with Asp178 in the binding pocket of SphK1, alteration of the aryl sulphonyl moiety changes the selectivity for SphK1 and SphK2. In this regard, the authors introduced various lipophilic substituents (i.e., alkyl, aryl, alkoxy, etc.) to the scaffold of compound **117** in place of the aryl sulphonyl moiety to mimic the sphingosine substrate of SphK1 and SphK2. The dodecyl analogue **118** proved to be the most potent dual SphK1/SphK2 inhibitor (SphK1 K_i = 0.679 μ M, SphK2 K_i = 0.951 μ M) compared with derivatives with a shorter alkyl tail. On the other hand, the diaryl ether, alkoxy, alkenyl, alkynyl analogues (structures not shown) showed no improvement in biological activity. Molecular docking studies highlighted that compound **118** fitted in the Sph binding pocket of SphK1 establishing hydrogen bonding of the 2-(hydroxymethyl)pyrrolidine moiety. Specifically, (1) the primary alcohol hydrogen bonded with Ser168 and (2) the tertiary nitrogen hydrogen bonded with Asp178. Similarly, hydrogen bonds between the pyrrolidine nitrogen and Asp308 as well as the hydroxyl group and Ser298 were observed in the homology model of SphK2 docked with **118**. The aliphatic dodecyl alkyl tail of compound **118** acquires a specific “J-shape”, generating hydrophobic interactions within the binding pocket of the enzyme.

Recently, Frydrych et al. [83] used commercially available D- and L-prolinol as the starting material for the synthesis of novel antimalarial agents, yielding new chiral compounds in which a pyrrolidine ring is incorporated in the linker connecting the

purine base to the phosphonate group(s) (**119a,b** and **120a,b**) (Fig. 24). Compounds **119a,b** and **120a,b** were evaluated as inhibitors of the plasmodial hypoxanthine-guanine-(xanthine)-phosphoribosyltransferase [HG(X)PRT] of *Plasmodium falciparum*, *P. vivax* (HGPRT) and human HGPRT, and the results were compared with those of the previously published inhibitors **123**, **124**, **125a,b** (Fig. 24). The biological results did not show an improvement in activity over compounds **123**, **124**, **125a,b**. In fact, the new nucleotide analogues had K_i values in the range between 9 and > 50 mM for human HGPRT, 5–44 mM for *Pf*HGXPT and between 20 and > 50 mM for *Pv*HGPRT, despite the increased flexibility achieved by the implementation of a CH_2 group between the nucleobase and the pyrrolidine ring, which allows a free rotation. The same results were obtained when replacing the pyrrolidine nucleus with a six membered-ring, such as piperidine or piperazine (structures not showed). However, the phosphoramidate prodrugs **121a,b** and **122a,b** (Fig. 24), exhibited good antimalarial activity in a *P. falciparum*-infected human erythrocyte assay. In particular, the bisphosphoramidate prodrug **122a** was potent ($\text{IC}_{50} = 2.5 \mu\text{M}$) against the chloroquine resistant *P. falciparum* W2 strain, with low cytotoxicity in human hepatocellular liver carcinoma (HepG2) and normal human dermal fibroblasts (NHDF) cell lines at a concentration of 100 μM .

5 Concluding Remarks

The present review is intended to provide significant support to medicinal chemists in the discovery of new biologically active pyrrolidine derivatives, providing a general overview of recent research concerning this scaffold, offering quick identification of the best synthetic route to apply. From this work, pyrrolidine emerges as a versatile scaffold found in molecules that exhibit a broad spectrum of biological activities. Pyrrolidines are useful to build compounds for fighting cancer and microbial infections, for metabolic diseases, as agents active in the CNS and for neurodegenerative diseases and immune disorders. Since three-dimensionality is an essential element of ligand–target interactions, the stereocenters present in pyrrolidine scaffolds would allow medicinal chemists to develop molecules with the most suitable configurations to fit into the ligand binding site of a target protein. In order to discover structurally novel compounds, the scaffold hopping strategy could be applied to the pyrrolidine core while maintaining its stereochemistry, together with exploration of the SAR of the most active pyrrolidine derivatives. We believe that the chemical versatility of the pyrrolidine nucleus and its ability to generate structural diversity could be essential to establish the clinical success of new bioactive molecules.

Funding Open access funding provided by Università degli Studi di Palermo within the CRUI-CARE Agreement. No funding was received to assist with the preparation of this manuscript.

Declarations

Conflict of Interest The authors declare that they have no known competing financial interests or personal relationships that could have appeared to influence the work reported in this paper.

Open Access This article is licensed under a Creative Commons Attribution 4.0 International License, which permits use, sharing, adaptation, distribution and reproduction in any medium or format, as long as you give appropriate credit to the original author(s) and the source, provide a link to the Creative Commons licence, and indicate if changes were made. The images or other third party material in this article are included in the article's Creative Commons licence, unless indicated otherwise in a credit line to the material. If material is not included in the article's Creative Commons licence and your intended use is not permitted by statutory regulation or exceeds the permitted use, you will need to obtain permission directly from the copyright holder. To view a copy of this licence, visit <http://creativecommons.org/licenses/by/4.0/>.

References

1. Raimondi MV, Presentato A, Li Petri G et al (2020) New synthetic nitro-pyrrolomycins as promising antibacterial and anticancer agents. *Antibiotics* 9:292. <https://doi.org/10.3390/antibiotic9060292>
2. Raimondi MV, Listro R, Cusimano MG et al (2019) Pyrrolomycins as antimicrobial agents. Microwave-assisted organic synthesis and insights into their antimicrobial mechanism of action. *Bioorg Med Chem* 27:721–728. <https://doi.org/10.1016/j.bmc.2019.01.010>
3. Spanò V, Rocca R, Barreca M et al (2020) Pyrrolo[2',3':3,4]cyclohepta[1,2-d][1,2]oxazoles, a new class of antimitotic agents active against multiple malignant cell types. *J Med Chem* 63:12023–12042. <https://doi.org/10.1021/acs.jmedchem.0c01315>
4. Cascioferro S, Maggio B, Raffa D et al (2016) A new class of phenylhydrazinylidene derivatives as inhibitors of *Staphylococcus aureus* biofilm formation. *Med Chem Res* 25:870–878. <https://doi.org/10.1007/s00044-016-1535-9>
5. Whatmore JL, Swann E, Barraja P et al (2002) Comparative study of isoflavone, quinoxaline and oxindole families of anti-angiogenic agents. *Angiogenesis* 5:45–51. <https://doi.org/10.1023/a:1021528628524>
6. Jampilek J (2019) Heterocycles in medicinal chemistry. *Molecules* 24:213839. <https://doi.org/10.3390/molecules24213839>
7. Gomtsyan A (2012) Heterocycles in drugs and drug discovery. *Chem Heterocycl Comp* 48:7–10. <https://doi.org/10.1007/s10593-012-0960-z>
8. Brown DG, Boström J (2016) Analysis of past and present synthetic methodologies on medicinal chemistry: where have all the new reactions gone? *J Med Chem* 59:4443–4458. <https://doi.org/10.1021/acs.jmedchem.5b01409>
9. Everett SA, Naylor MA, Barraja P et al (2001) Controlling the rates of reductively-activated elimination from the (indol-3-yl)methyl position of indolequinones. *J Chem Soc Perkin Trans* 2:843–860. <https://doi.org/10.1039/B009652K>
10. Clemons PA, Wilson JA, Dančák V et al (2011) Quantifying structure and performance diversity for sets of small molecules comprising small-molecule screening collections. *Proc Natl Acad Sci USA* 108:6817–6822. <https://doi.org/10.1073/pnas.1015024108>
11. Lovering F, Bikker J, Humblet C (2009) Escape from flatland: increasing saturation as an approach to improving clinical success. *J Med Chem* 52:6752–6756. <https://doi.org/10.1021/jm901241e>
12. Aldeghi M, Malhotra S, Selwood DL, Chan AWE (2014) Two- and three-dimensional rings in drugs. *Chem Biol Drug Des* 83:450–461. <https://doi.org/10.1111/cbdd.12260>
13. Ritchie TJ, Macdonald SJF, Peace S et al (2012) The developability of heteroaromatic and heteroaliphatic rings—do some have a better pedigree as potential drug molecules than others? *Med Chem Commun* 3:1062–1069. <https://doi.org/10.1039/C2MD20111A>
14. Goldberg FW, Kettle JG, Kogej T et al (2015) Designing novel building blocks is an overlooked strategy to improve compound quality. *Drug Discov Today* 20:11–17. <https://doi.org/10.1016/j.drudis.2014.09.023>
15. Tajabadi FM, Campitelli MR, Quinn RJ (2013) Scaffold flatness: reversing the trend. *Springer Sci Rev* 1:141–151. <https://doi.org/10.1007/s40362-013-0014-7>
16. Maier ME (2015) Design and synthesis of analogues of natural products. *Org Biomol Chem* 13:5302–5343. <https://doi.org/10.1039/C5OB00169B>

17. Liu XC, Lai D, Liu QZ et al (2016) Bioactivities of a new pyrrolidine alkaloid from the root barks of *Orixa japonica*. *Molecules*. <https://doi.org/10.3390/molecules21121665>
18. Carroll FI (2009) Epibatidine analogs synthesized for characterization of nicotinic pharmacophores—a review. *Heterocycles* 79:99–120
19. Islam MT, Mubarak MS (2020) Pyrrolidine alkaloids and their promises in pharmacotherapy. *Adv Tradit Med* 20:13–22. <https://doi.org/10.1007/s13596-019-00419-4>
20. Bhat C, Tilve SG (2014) Recent advances in the synthesis of naturally occurring pyrrolidines, pyrrolizidines and indolizidine alkaloids using proline as a unique chiral synthon. *RSC Adv* 4:5405–5452. <https://doi.org/10.1039/C3RA44193H>
21. Vitaku E, Smith DT, Njardarson JT (2014) Analysis of the structural diversity, substitution patterns, and frequency of nitrogen heterocycles among US FDA Approved Pharmaceuticals. *J Med Chem* 57:10257–10274. <https://doi.org/10.1021/jm501100b>
22. Dalko PI, Moisan L (2004) In the golden age of organocatalysis. *Angew Chem Int Ed* 43:5138–5175. <https://doi.org/10.1002/anie.200400650>
23. Higashiyama K, Inoue H, Takahashi H (1994) Diastereoselective addition of chiral imines and 1,3-oxazolidines with grignard reagents; asymmetric synthesis of (R)-2-aryl- and (R, R)-2,5-bis(aryl)pyrrolidines. *Tetrahedron* 50:1083–1092. [https://doi.org/10.1016/S0040-4020\(01\)80819-X](https://doi.org/10.1016/S0040-4020(01)80819-X)
24. Llopis S, García T, Cantín Á et al (2018) Chiral hybrid materials based on pyrrolidine building units to perform asymmetric Michael additions with high stereocontrol. *Catal Sci Technol* 8:5835–5847. <https://doi.org/10.1039/C8CY01650J>
25. Henary M, Kananda C, Rotolo L et al (2020) Benefits and applications of microwave-assisted synthesis of nitrogen containing heterocycles in medicinal chemistry. *RSC Adv* 10:14170–14197. <https://doi.org/10.1039/D0RA01378A>
26. Li Petri G, Spanò V, Spatola R et al (2020) Bioactive pyrrole-based compounds with target selectivity. *Eur J Med Chem* 208:112783. <https://doi.org/10.1016/j.ejmech.2020.112783>
27. Cascioferro S, Raimondi MV, Cusimano MG et al (2015) Pharmaceutical potential of synthetic and natural pyrrolomycins. *Molecules* 20:21658–21671. <https://doi.org/10.3390/molecules201219797>
28. Raimondi MV, Schillaci D, Petruso S (2007) Synthesis and anti-staphylococcal activity of new halogenated pyrroles related to Pyrrolomycins F. *J Heterocycl Chem* 44:1407–1411. <https://doi.org/10.1002/jhet.5570440626>
29. Adrio J, Carretero JC (2019) Stereochemical diversity in pyrrolidine synthesis by catalytic asymmetric 1,3-dipolar cycloaddition of azomethine ylides. *Chem Commun* 55:11979–11991. <https://doi.org/10.1039/C9CC05238K>
30. Biswas AK, Johnson DG (2012) Transcriptional and nontranscriptional functions of E2F1 in response to DNA damage. *Cancer Res* 72:13–17. <https://doi.org/10.1158/0008-5472.CAN-11-2196>
31. Gupta MR, Thakur K, Khare NK (2018) L-Proline/CeCl₃·7H₂O-Nal mediated stereoselective synthesis of α-2-deoxy glycosides from glucal. *Carbohydr Res* 457:51–55. <https://doi.org/10.1016/j.carres.2018.01.003>
32. Brooks WH, Guida WC, Daniel KG (2011) The significance of chirality in drug design and development. *Curr Top Med Chem* 11:760–770. <https://doi.org/10.2174/156802611795165098>
33. Kunitski M, Riehn C, Matylitsky V et al (2010) Pseudorotation in pyrrolidine: rotational coherence spectroscopy and ab initio calculations of a large amplitude intramolecular motion. *Phys Chem Chem Phys* 12:72–81. <https://doi.org/10.1039/B917362E>
34. Galloway WRJD, Isidro-Llobet A, Spring DR (2010) Diversity-oriented synthesis as a tool for the discovery of novel biologically active small molecules. *Nat Commun* 1:80. <https://doi.org/10.1038/ncomms1081>
35. Kumar A, Gupta G, Srivastava S (2010) Diversity oriented synthesis of pyrrolidines via natural carbohydrate solid acid catalyst. *J Comb Chem* 12:458–462. <https://doi.org/10.1021/cc100007a>
36. Koskinen AMP, Helaja J, Kumpulainen ETT et al (2005) Locked conformations for proline pyrrolidine ring: synthesis and conformational analysis of cis- and trans-4-tert-butylprolines. *J Org Chem* 70:6447–6453. <https://doi.org/10.1021/jo050838a>
37. Jurica EA, Wu X, Williams KN et al (2017) Discovery of pyrrolidine-containing GPR40 agonists: stereochemistry effects a change in binding mode. *J Med Chem* 60:1417–1431. <https://doi.org/10.1021/acs.jmedchem.6b01559>
38. Luxenburger A, Schmidt D, Ianes C et al (2019) Design, synthesis and biological evaluation of isoxazole-based CK1 inhibitors modified with chiral pyrrolidine scaffolds. *Molecules* 24:873. <https://doi.org/10.3390/molecules24050873>

39. Fanning SW, Hodges-Gallagher L, Myles DC et al (2018) Specific stereochemistry of OP-1074 disrupts estrogen receptor alpha helix 12 and confers pure antiestrogenic activity. *Nat Commun* 9:2368. <https://doi.org/10.1038/s41467-018-04413-3>
40. Jiang B, Duan JJ-W, Stachura S et al (2020) Discovery of (3*S*,4*S*)-3-methyl-3-(4-fluorophenyl)-4-(4-(1,1,1,3,3,3-hexafluoro-2-hydroxyprop-2-yl)phenyl)pyrrolidines as novel ROR γ t inverse agonists. *Bioorg Med Chem Lett* 30:127392. <https://doi.org/10.1016/j.bmcl.2020.127392>
41. An F, Maji B, Min E et al (2020) Basicities and nucleophilicities of pyrrolidines and imidazolidinones used as organocatalysts. *J Am Chem Soc* 142:1526–1547. <https://doi.org/10.1021/jacs.9b11877>
42. Breugst M, Reissig H-U (2020) The Huisgen reaction: milestones of the 1,3-dipolar cycloaddition. *Angew Chem Int Ed* 59:12293–12307. <https://doi.org/10.1002/anie.202003115>
43. Maiuolo L, Algieri V, Olivito F, De Nino A (2020) Recent developments on 1,3-dipolar cycloaddition reactions by catalysis in green solvents. *Catalysts* 10:65. <https://doi.org/10.3390/catal10010065>
44. Coldham I, Hufton R (2005) Intramolecular dipolar cycloaddition reactions of azomethine ylides. *Chem Rev* 105:2765–2810. <https://doi.org/10.1021/cr040004c>
45. Min R, Wu W, Wang M et al (2019) Discovery of 2-(1-(3-(4-Chloroxyphenyl)-3-oxo-propyl)pyrrolidine-3-yl)-1H-benzo[d]imidazole-4-carboxamide: a potent poly(ADP-ribose) polymerase (PARP) inhibitor for treatment of cancer. *Molecules* 24:1901. <https://doi.org/10.3390/molecules24101901>
46. Wang Y, Zhao H, Brewer JT et al (2018) De Novo design, synthesis, and biological evaluation of 3,4-disubstituted pyrrolidine sulfonamides as potent and selective glycine transporter 1 competitive inhibitors. *J Med Chem* 61:7486–7502. <https://doi.org/10.1021/acs.jmedchem.8b00295>
47. Zhang H, Ding CZ, Lai Z et al (2015) Synthesis and biological evaluation of novel pyrrolidine acid analogs as potent dual PPAR α/γ agonists. *Bioorg Med Chem Lett* 25:1196–1205. <https://doi.org/10.1016/j.bmcl.2015.01.066>
48. Periyasami G, Kamalraj S, Padmanaban R et al (2019) Glucosamine-6-phosphate synthase inhibiting C3- β -cholesterol tethered spiro heterocyclic conjugates: synthesis and their insight of DFT and docking study. *Bioorg Chem* 88:102920. <https://doi.org/10.1016/j.bioorg.2019.102920>
49. Shyamsivappan S, Saravanan A, Vivek R et al (2020) Novel phenyl and thiophene dispiro indenoquinoxaline pyrrolidine quinolones induced apoptosis via G1/S and G2/M phase cell cycle arrest in MCF-7 cells. *New J Chem* 44:15031–15045. <https://doi.org/10.1039/D0NJ02588G>
50. Benabdallah M, Talhi O, Nouali F et al (2018) Advances in spirocyclic hybrids: chemistry and medicinal actions. *Curr Med Chem* 25:3748–3767. <https://doi.org/10.2174/0929867325666180309124821>
51. Hati S, Tripathy S, Dutta PK et al (2016) Spiro[pyrrolidine-3, 3'-oxindole] as potent anti-breast cancer compounds: their design, synthesis, biological evaluation and cellular target identification. *Sci Rep* 6:1–10. <https://doi.org/10.1038/srep32213>
52. Guazzelli L, D'Andrea F, Sartini S et al (2019) Synthesis and investigation of polyhydroxylated pyrrolidine derivatives as novel chemotypes showing dual activity as glucosidase and aldose reductase inhibitors. *Bioorg Chem* 92:103298. <https://doi.org/10.1016/j.bioorg.2019.103298>
53. Li Z, Wang X, Lin Y et al (2020) Design, synthesis, and evaluation of pyrrolidine based CXCR4 antagonists with in vivo anti-tumor metastatic activity. *Eur J Med Chem* 205:112537. <https://doi.org/10.1016/j.ejmech.2020.112537>
54. da Silva EC, Yamakawa NCG, Santos AAD, Coelho F (2017) Short and diastereoselective total synthesis of the polyhydroxylated pyrrolidine LAB-1: a potent α -glycosidase inhibitor. *Synth* 49:4869–4875. <https://doi.org/10.1055/s-0036-1590799>
55. Debbabi KF, Al-Harbi SA, Al-Saidi HM et al (2016) Study of reactivity of cyanoacetohydrazonoethyl-*N*-ethyl-*N*-methyl benzenesulfonamide: preparation of novel anticancer and antimicrobial active heterocyclic benzenesulfonamide derivatives and their molecular docking against dihydrofolate reductase. *J Enzym Inhib Med Ch* 31:7–19. <https://doi.org/10.1080/14756366.2016.1217851>
56. Rybka S, Obniska J, Rapacz A et al (2017) Synthesis and evaluation of anticonvulsant properties of new *N*-Mannich bases derived from pyrrolidine-2,5-dione and its 3-methyl-, 3-isopropyl, and 3-benzhydryl analogs. *Bioorg Med Chem Lett* 27:1412–1415. <https://doi.org/10.1016/j.bmcl.2017.02.002>
57. Rybka S, Obniska J, Żmudzki P et al (2017) Synthesis and determination of lipophilicity, anticonvulsant activity, and preliminary safety of 3-substituted and 3-unsubstituted *N*-[(4-aryl)piperazin-1-yl]alkyl]pyrrolidine-2,5-dione derivatives. *ChemMedChem* 12:1848–1856. <https://doi.org/10.1002/cmdc.201700539>

58. Góra M, Czopek A, Rapacz A et al (2020) Synthesis, anticonvulsant and antinociceptive activity of new hybrid compounds: derivatives of 3-(3-methylthiophen-2-yl)-pyrrolidine-2,5-dione. *Int J Mol Sci* 21:5750. <https://doi.org/10.3390/ijms21165750>
59. Obniska J, Góra M, Rapacz A et al (2021) Synthesis, anticonvulsant, and antinociceptive activity of new 3-(3-methyl-2,5-dioxo-3-phenylpyrrolidin-1-yl)propanamides and 3-phenyl-butanamides. *Arch Pharm (Weinheim)* 354:e2000225. <https://doi.org/10.1002/ardp.202000225>
60. Góra M, Czopek A, Rapacz A et al (2021) Design, synthesis and biological activity of new amides derived from 3-benzhydryl and 3-sec-butyl-2,5-dioxo-pyrrolidin-1-yl-acetic acid. *ChemMedChem* 16:1619–1630. <https://doi.org/10.1002/cmdc.202001007>
61. Oktay K, Kose L, Şendil K et al (2017) Synthesis of 3-chloro-1-substituted aryl pyrrolidine-2,5-dione derivatives: discovery of potent human carbonic anhydrase inhibitors. *Med Chem Res*. <https://doi.org/10.1007/s00044-017-1865-2>
62. Jan MS, Ahmad S, Hussain F et al (2020) Design, synthesis, in-vitro, in-vivo and in-silico studies of pyrrolidine-2,5-dione derivatives as multitarget anti-inflammatory agents. *Eur J Med Chem* 186:111863. <https://doi.org/10.1016/j.ejmech.2019.111863>
63. Gouda AM, Ali HI, Almalki WH et al (2016) Design, synthesis, and biological evaluation of some novel pyrrolizine derivatives as COX inhibitors with anti-inflammatory/analgesic activities and low ulcerogenic liability. *Molecules* 21:201. <https://doi.org/10.3390/molecules21020201>
64. Pannala P, Reddy P, Misra S et al (2017) Synthesis, molecular docking, in vitro antiproliferative and antioxidant activity of novel pyrrolidinyl-carbazole derivatives. *Curr Org Synth* 14:1172–1179. <https://doi.org/10.2174/1570179414666170606120934>
65. Aboul-Enein M, El-Azzouny AAE-S, Saleh OA et al (2016) Synthesis, bio-evaluation and molecular modeling studies of (2S)-1-[[[1-substituted cyclohexyl] methyl] amino] acetyl] pyrrolidine-2-carbonitriles for their DPP-4 inhibiting activity. *Int J Pharm Sci Rev Res* 39:230–240 (scopus ID: 19700188319)
66. Wan Y, Wang J, Sun F et al (2015) Design, synthesis and preliminary biological studies of pyrrolidine derivatives as Mcl-1 inhibitors. *Bioorg Med Chem* 23:7685–7693. <https://doi.org/10.1016/j.bmc.2015.11.014>
67. Gerokonstantis DT, Nikolaou A, Magkrioti C et al (2020) Synthesis of novel 2-pyrrolidinone and pyrrolidine derivatives and study of their inhibitory activity against autotaxin enzyme. *Bioorg Med Chem* 28:115216. <https://doi.org/10.1016/j.bmc.2019.115216>
68. Odusami JA, Ikhile MI, Izunobi JU et al (2020) Synthesis of substituted N-(2'-nitrophenyl) pyrrolidine-2-carboxamides towards the design of proline-rich antimicrobial peptide mimics to eliminate bacterial resistance to antibiotics. *Bioorg Chem* 105:104340. <https://doi.org/10.1016/j.bioorg.2020.104340>
69. De Tran Q, Bepary S, Lee GH et al (2016) Synthesis of (3S,4S)-4-aminopyrrolidine-3-ol derivatives and biological evaluation for their BACE1 inhibitory activities. *Bioorg Med Chem Lett* 26:51–54. <https://doi.org/10.1016/j.bmcl.2015.11.033>
70. Choubey PK, Tripathi A, Sharma P, Shrivastava SK (2020) Design, synthesis, and multitargeted profiling of N-benzylpyrrolidine derivatives for the treatment of Alzheimer's disease. *Bioorg Med Chem* 28:115721. <https://doi.org/10.1016/j.bmc.2020.115721>
71. Bashandy M, El-Gilil S (2016) Synthesis, molecular docking and antihuman breast cancer activities of novel thiazolyl acetoneitriles and thiazolyl acrylonitriles and their derivatives containing benzenesulfonylpyrrolidine moiety. *Heterocycles* 92:431–469. <https://doi.org/10.3987/COM-15-13384>
72. Hassan AHE, Park HR, Yoon YM et al (2019) Antiproliferative 3-deoxysphingomyelin analogs: design, synthesis, biological evaluation and molecular docking of pyrrolidine-based 3-deoxysphingomyelin analogs as anticancer agents. *Bioorg Chem* 84:444–455. <https://doi.org/10.1016/j.bioorg.2018.11.040>
73. Zhang H, Wang X, Mao J et al (2018) Synthesis and biological evaluation of novel benzofuran-based pyrrolidine hydroxamates as matrix metalloproteinase inhibitors with nitric oxide releasing activity. *Bioorg Med Chem* 26:4363–4374. <https://doi.org/10.1016/j.bmc.2018.06.023>
74. Asano M, Hitaka T, Imada T et al (2017) Synthesis and biological evaluation of novel selective androgen receptor modulators (SARMs). Part II: Optimization of 4-(pyrrolidin-1-yl)benzoxonitrile derivatives. *Bioorg Med Chem Lett* 27:1897–1901. <https://doi.org/10.1016/j.bmcl.2017.03.038>
75. Aikawa K, Miyawaki T, Hitaka T et al (2015) Synthesis and biological evaluation of novel selective androgen receptor modulators (SARMs). Part I. *Bioorg Med Chem* 23:2568–2578. <https://doi.org/10.1016/j.bmc.2015.03.032>

76. Kaur S, Kumari P, Singh G et al (2018) Design and synthesis of aza-/oxa heterocycle-based conjugates as novel anti-inflammatory agents targeting cyclooxygenase-2. *ACS Omega* 3:5825–5845. <https://doi.org/10.1021/acsomega.8b00445>
77. Zhou P, Xiang L, Zhao D et al (2019) Synthesis, biological evaluation, and structure activity relationship (SAR) study of pyrrolidine amide derivatives as *N*-acylethanolamine acid amidase (NAAA) inhibitors. *Med Chem Commun* 10:252–262. <https://doi.org/10.1039/C8MD00432C>
78. Lucescu L, Ghinet A, Shova S et al (2019) Exploring isoxazoles and pyrrolidinones decorated with the 4,6-dimethoxy-1,3,5-triazine unit as human farnesyltransferase inhibitors. *Arch Pharm* 352:1800227. <https://doi.org/10.1002/ardp.201800227>
79. Kumar A, Singh UK, Muzaffar F et al (2018) Design, synthesis and anti-proliferative activity of novel 1,2,4-triazine and pyrrolidin-2-one derivatives. *Der Pharma Chemica* 10(1):124–131
80. Rezaei M, Bayrak Ç, Taslimi P et al (2018) The first synthesis and antioxidant and anticholinergic activities of 1-(4,5-dihydroxybenzyl)pyrrolidin-2-one derivative bromophenols including natural products. *Turk J Chem* 42:808–825. <https://doi.org/10.3906/kim-1709-34>
81. Tilekar K, Upadhyay N, Meyer-Almes F-J et al (2020) Synthesis and biological evaluation of pyrazoline and pyrrolidine-2,5-dione hybrids as potential antitumor agents. *ChemMedChem* 15:1813–1825. <https://doi.org/10.1002/cmdc.202000458>
82. Li H, Sibley CD, Kharel Y et al (2021) Lipophilic tail modifications of 2-(hydroxymethyl)pyrrolidine scaffold reveal dual sphingosine kinase 1 and 2 inhibitors. *Bioorg Med Chem* 30:115941. <https://doi.org/10.1016/j.bmc.2020.115941>
83. Frydrych J, Keough DT, Chavchich M et al (2021) Nucleotide analogues containing a pyrrolidine, piperidine or piperazine ring: synthesis and evaluation of inhibition of plasmodial and human 6-oxopurine phosphoribosyltransferases and in vitro antimalarial activity. *Eur J Med Chem* 219:113416. <https://doi.org/10.1016/j.ejmech.2021.113416>

Publisher's Note Springer Nature remains neutral with regard to jurisdictional claims in published maps and institutional affiliations.

Authors and Affiliations

Giovanna Li Petri¹ · Maria Valeria Raimondi¹  · Virginia Spanò¹ · Ralph Holl² · Paola Barraja¹ · Alessandra Montalbano¹

¹ Department of Biological, Chemical and Pharmaceutical Sciences and Technologies (STEBICEF), University of Palermo, Via Archirafi 32, 90123 Palermo, Italy

² Department of Chemistry, Institute of Organic Chemistry, University of Hamburg, Martin-Luther-King-Platz 6, 20146 Hamburg, Germany